Current Research in Toxicology 3 (2022) 100064

Contents lists available at ScienceDirect

Current Research in Toxicology

journal homepage: www.elsevier.com/locate/crtox

Use of computational toxicology tools to predict *in vivo* endpoints associated with Mode of Action and the endocannabinoid system: A case study with chlorpyrifos, chlorpyrifos-oxon and $^{\Delta 9}$Tetrahydrocannabinol

Marilyn Silva [a,*], Ryan Kin-Hin Kwok [b]

[a] *Retired from California Environmental Protection Agency with a Career in Toxicology and Risk Assessment, United States*
[b] *Independent Researcher, United States*

ARTICLE INFO

Keywords:
Chlorpyrifos
Chlorpyrifos-oxon
$^{\Delta 9}$Tetrahydrocannabinol
High throughput toxicokinetics
HTTK-Pop
ToxCast/Tox21

ABSTRACT

Currently, there is a lack of knowledge about the effects of co-exposures of cannabis, contaminated with pesticides like chlorpyrifos (CPF) and the toxic metabolite CPF-oxon (CPFO). CPF/CPFO residues, and $^{\Delta 9}$Tetrahydrocannabinol ($^{\Delta 9}$THC), the main component in cannabis, are known to disrupt the endocannabinoid system (eCBS) resulting in neurodevelopmental defects. Although there are *in vivo* data characterizing CPF/CPFO and $^{\Delta 9}$THC, there are mechanistic data gaps and deficiencies. In this study, an investigation of open access CompTox tools and ToxCast/Tox21 data was performed to determine targets relating to the modes of action (MOA) for these compounds and, given the available biological targets, predict points of departure (POD). The main findings were as follows: 1) *In vivo* PODs for each chemical were from open literature, 2) Concordance between ToxCast/Tox21 assay targets and known targets in the metabolic and eCBS pathways was evaluated, 3) Human Equivalent Administered Dose (EAD_{Human}) PODs showed the High throughput toxicokinetic (HTTK) 3 compartment model (3COMP) was more predictive of *in vivo* PODs than the PBTK model for CPF, CPFO and $^{\Delta 9}$THC, 4) Age-adjusted 3COMP HTTK-Pop EAD_{Human}, with CPF and CPFO ToxCast/Tox21 AC_{50} values as inputs were predictive for ages 0–4 when but not $^{\Delta 9}$THC compared to *in vivo* PODs. 5) Age-related refinements for CPF/CPFO were primarily from ToxCast/Tox21 active hit-calls for nuclear receptors, CYP2B6 and AChE inhibition (CPFO only) associated with the metabolic pathway. Only one assay target (aryl-hydrocarbon hydroxylase receptor) was common between CPF/CPFO and $^{\Delta 9}$THC. While computational refinements may select some sensitive events involved in the metabolic pathways; this is highly dependent on the cytotoxicity limits, availability of metabolic activity in the ToxCast/Tox21 assays and reliability of assay performance. Some uncertainties and data gaps for $^{\Delta 9}$THC might be addressed with assays specific to the eCBS. For CPF, assays with appropriate metabolic activation could better represent the toxic pathway.

1. Introduction

Medicinal and recreational cannabis has increased globally by 60% in 2019 to over 275 million people using marijuana worldwide in 2021 (https://www.unodc.org/unodc/press/releases/2021/accessed1/2022) (DBH, 2022). Cannabis consumption occurs through diverse routes (inhaled smoke, vaping of liquid extracts, resins or waxes, lotions, edibles) (Raber et al., 2015). The primary component in cannabis is the psychoactive delta-9-tetrahydrocannabinol ($^{\Delta 9}$THC) (ElSohly, 2002). $^{\Delta 9}$THC is rapidly absorbed in lungs (Musshoff and Madea, 2006) and is highly concentrated in human breast milk (EFSA, 2015, Baker et al., 2018). Further, $^{\Delta 9}$THC has neurodevelopmental effects in rodents and humans that lead to long term decrements in behavior, cognition, locomotor activity, birth weights and numerous other effects (Miller et al., 2019, de Salas-Quiroga et al., 2020, Zamberletti and Rubino, 2021, Slotkin et al., 2020, Fergusson et al., 2002). Cannabis smoke was listed a reproductive toxicant January 3, 2020, under Proposition 65 in California (epidemiological studies reviewed in: OEHHA (2019); https://oehha.ca.gov/proposition-65/proposition-65-list/; accessed 1-2022).

While at least half of the United States has legalized medicinal and/or recreational cannabis the use of pesticides on cannabis crops is

Abbreviations: Pop, Population; HTTK:, High throughput toxicokinetics; ToxCast/Tox21, CompTox Chemicals Dashboard High throughput Assays.

* Corresponding author at: 2437 Evenstar Lane, Davis, California 95616, United States.
E-mail address: marilynhelensilva@gmail.com (M. Silva).

https://doi.org/10.1016/j.crtox.2022.100064
Received 13 August 2021; Revised 16 January 2022; Accepted 3 February 2022

unregulated because it is not federally recognized as a legal crop (USEPA; https://www.epa.gov/pesticide-tolerances; accessed 7-2021). Pesticide use includes the organophosphate insecticides, including chlorpyrifos (CPF, ethyl), malathion and dichlorvos, which have detectable residues in cannabis plants and products (Taylor and Birkett, 2020, Voelker and Holmes, 2015). Residues are especially prevalent in cannabis sold on the black market without stringent quality control, or quality assurance (Stempfer et al., 2021, Wylie et al., 2020, Dryburgh et al., 2018). Not all states that legally sell cannabis require testing before sales, and even when testing is required, regulations offer varying levels of safety (Seltenrich, 2019). CPF and the main metabolite CPF-oxon (CPFO) are neurotoxic through inhibition of acetylcholinesterase (AChE) in plasma, red blood cells (RBC) and brain, leading to cholinergic symptoms in the peripheral and central nervous systems (Casida, 2017). It has been extensively used in agricultural settings throughout much of the United States and internationally (CDPR, 2018, EFSA, 2014). CPF is highly lipophilic and is readily absorbed through the placenta and into fetal tissues, including brain, during development (El-Masri et al., 2016). CPF is transferred to nursing infants or neonates through the milk (Weldon et al., 2011). There are numerous epidemiological studies describing associations between CPF exposure during pregnancy or early childhood and effects on learning and behavior (Rauh et al., 2015, Rauh et al., 2012), including developmental delays related to cognition and motor function, attention deficit hyperactivity disorder, autism spectrum disorder (ASD) and tremors (Shelton et al., 2014) associated with very low *in utero* CPF exposures. Many of the cognitive and behavioral effects observed from CPF exposure are also observed after human and rodent exposure to $^{\Delta 9}$THC during development (Newsom and Kelly, 2008, Trezza et al., 2008).

2. Theory

Human health concerns involve the fact that CPF, CPFO and $^{\Delta 9}$THC have in common their effects on the endocannabinoid system (eCBS) discovered in the 1990 s while investigating the $^{\Delta 9}$THC Mode of Action (MOA)[1] (Liu et al., 2015, Nomura et al., 2008, Medina-Cleghorn et al., 2014, Carr et al., 2020, Di Marzo, 2011, Di Marzo et al., 2008). It is generally comprised of (1) the G-protein-coupled receptors (GPCR) interacting with cannabinoid 1 (CB1) and CB2 receptors coupled to the $Gi_{/o}$ proteins (Lüscher and Ungless, 2006) which are the most abundant in the central nervous system (CNS) (Berghuis et al., 2007) or immune cells and tissues (Pertwee, 2006), respectively; (2) two principal endogenous ligands (2-arachidonoylglycerol (2-AG) and anandamide (AEA); and (3) the serine hydrolases monoacylglycerol lipase (MAGL), and fatty acid amide hydrolase (FAAH) (Di Marzo et al., 2011), as well as other signaling pathways (Berghuis et al., 2007). The eCBS helps to shape neuronal connectivity in the brain throughout development and into adulthood (Mato et al., 2003), including the GABAergic, glutamatergic, opioid, and dopaminergic systems (Zou and Kumar, 2018).

While CPF/CPFO and $^{\Delta 9}$THC are agonists at the CB1 receptor, CPF and CPFO also act by inhibiting FAAH and MAGL preventing AEA and 2-AG breakdown (Carr et al., 2017, Di Marzo, 2011, Carr et al., 2020). Cellular build-up of eCBs results in inhibited release of critical neurotransmitters (glutamate, ɣ-amino-butyric acid (GABA) and dopamine) at neuronal synapses and subsequent neurotoxicity (Zou and Kumar, 2018). Further, a strong connection between eCB and opioid systems in the fetal brain are negatively affected by $^{\Delta 9}$THC exposure leading to behavioral and emotional decrements in later life (Wang et al., 2006).

[1] Mode of Action (MOA) was defined in a footnote as follows: From a risk assessment perspective: "Mode of action reflects the key and obligatory steps through which a chemical interacts with the organism… And the organism's response. MOA is chemical-specific." (Contemporary Issues in Risk Assessment (toxicology.org); accessed 10/2021).

Historically, *in vivo* dose–response studies have been used to characterize CPF/CPFO and $^{\Delta 9}$THC effects on developmental neurotoxicity (Carr et al., 2017, Mohammed et al., 2018, O'Shea et al., 2006). However animal studies generally lack mechanistic data that could identify a molecular 'tipping point' where an organism may no longer adapt or recover from chemical insult (Frank et al., 2018). The US EPA cheminformatics-based, open access computational toxicology (CompTox) tools, as part of new approach methodologies (NAMs), were developed to supplement, support or even replace *in vivo* bioassays (Williams et al., 2017). Further, the US EPA Office of Chemical Safety and Pollution Prevention and the Office of Research and Development have been charged to "reduce requests for, and funding of mammal studies by 30% by 2025, and eliminate all mammal study requests by 2035," (US EPA, 2020b).

The primary CPF/CPFO and $^{\Delta 9}$THC Modes of Action (MOA)[1] are ***individually*** well documented, however, there are no animal study data on the combined toxicity of CPF and THC. Therefore, it was of interest to develop a predictive *in vivo* endpoint based on the signals from the ToxCast/Tox21 assays by comparing known mechanistic activities with those predicted through a series of increasingly refined CompTox tools. Examples of these tools are: (1) The Toxicity Forecaster and Tox21 (ToxCast/Tox21) database, available on the CompTox Chemicals Dashboard (CompTox Chemicals Dashboard | Home (epa.gov); accessed 10-2021), is comprised of hundreds of assays (Williams et al., 2017) that identify targets in metabolic pathways; (2) the Integrated Chemical Environment (ICE) 3 Compartment (3COMP) or Physiologically Based Toxicokinetic (PBTK) oral models incorporating the High-Throughput Toxicokinetics (HTTK R-package: https://CRAN.R-project.org/package=httk; Wambaugh et al. (2015a); Breen et al. (2021)) to calculate Equivalent Administered Dose in humans (EAD_{Human} mg/kg/day)(Pearce et al., 2017, Sipes et al., 2017, ICE, 2021, Bell et al., 2020); (3) The human population-based HTTK oral model that simulates internal doses by age using the Center for Disease Control National Health (CDC) and Nutrition Examination Survey (NHANES) data (Wambaugh et al., 2018, Ring et al., 2017).

Previous work reported a case study for prioritizing chemicals by compiling ToxCast/Tox21 data using all assays for each of 448 chemicals, estimating activities at the 50th (approximating a lowest-observed-effect levels: LOEL) and 95th percentile (approximating a no-observed-effect level: NOEL). These *in vitro* values were converted by *in vitro* to *in vivo* extrapolation (IVIVE) to predict PODs for potential use in risk assessment (Friedman et al., 2019). POD predictions were then compared to open assess *in vivo* LOEL/NOELs (Martin et al., 2009; Williams et al., 2017) compiled for each chemical to calculate PODs at the 5th percentile. The predictions were compared to the *in vivo* data. Their results indicated that the lowest chemical concentrations leading to *in vitro* bioactivities could potentially correspond to a threshold for downstream *in vivo* toxicity. Suggested next steps were to perform modifications of the IVIVE approach and refine the utility of their model.

This case study then used similar CompTox tools to estimate CPF/CPFO and $^{\Delta 9}$THC PODs focusing on *in vitro* targets in the known and/or presumptive Mode of Action (MOA) for comparison with measured *in vivo* points of departure (POD: mg/kg/day) relating to disruptions in the eCBS (Carr et al., 2020, Carr et al., 2017, Di Marzo, 2011, Huestis, 2005, Testai et al., 2010, Dinis-Oliveira, 2016). Hence, the goals were: (1) identifying areas of concordance between ToxCast/Tox21 assay targets and existing *in vivo* data relating to known metabolic pathways or common targets affecting eCBS pathways, (2) calculating EAD_{Human} via ICE (version 3.5) 3COMP and PBTK oral models to evaluate which model is most concordant with the *in vivo* PODs, (3) calculating oral age-adjusted HTTK-Pop EAD_{Human} using the most predictive HTTK model (i.e., 3COMP or PBTK) to see if the further refinement produces greater concordance with *in vivo* PODs; and (5) determining biological relevance of the findings in the context of risk assessment, based on the computational tools available.

3. Methods

3.1. Open access literature selection

The *in vivo* studies for each chemical were selected from open literature based on neurodevelopmental parameters related to the eCBS after CPF, CPFO and $^{\Delta 9}$THC treatment. The process involved selection of studies that: 1) were (as closely as possible) designed to investigate the effects of each chemical on parameters associated with the eCBS during development; 2) used standard strains of laboratory rat (i.e., Sprague-Dawley or Wistar); 3) used technical grade of administered chemicals, as was also used in the ToxCast/Tox21 assays; and 4) had lowest-observed-effect levels (LOEL) associated with the eCBS. The *in vivo* studies and LOELs provided the foundation for comparisons with the modeled predictions.

3.2. Interspecies scaling versus default interspecies extrapolation

The *in vivo* studies were performed in rodents, while the ToxCast/Tox21 assays used mainly human tissues/proteins. The HTTK 3COMP and multi-compartment PBTK and HTTK-Pop models used human toxicokinetic parameters from oral exposure to predict human EADs (Ring et al., 2017, Bell et al., 2018, Sipes et al., 2017, Wambaugh et al., 2015b, Wambaugh et al., 2018). To account for the interspecies (rat to human) toxicokinetics, allometric scaling (AS: 0.162) or a default interspecies extrapolation uncertainty factor (UF: 10-fold) were calculated for comparisons between EAD $_{\text{Human}}$ and *in vivo* rodent PODs (Eqs. (1) and (2)) (Nair and Jacob, 2016, WHO, 2017). While the interspecies extrapolations are not exact, they provided a conservative estimation of data uncertainty (WHO, 2017).

$$In\ Vivo\ \ Interspecies\ \ Allometrically\ Scaled\ LOEL\ or\ ELOEL\ Based\ on\ Body\ \ Weight\ \ = (AS\ \ LOEL\ \ or\ AS\ \ ELOEL)\ x\ (0.162) \quad (1)$$

$$In\ Vivo\ \ Interspecies\ \ Extrapolation\ \ = \frac{LOEL\ \ or\ \ ELOEL}{Default\ \ \ UF10} \quad (2)$$

3.3. ToxCast/Tox21 in vitro assays

ToxCast/Tox21 results on the CompTox Chemicals Dashboard characterized CPF, CPFO and $^{\Delta 9}$THC interactions with intended target families (e.g., DNA binding, CYP [P450s], receptor-ligand binding, etc.) and their biological molecular targets, as concentration at 50% maximum activity (AC_{50}) (Judson et al., 2011). These chemical interactions provided support for the known MOAs and mechanisms potentially related to the eCBS (e.g., ɣ-amino butyric acid [GABA], dopamine or opioid receptors). ToxCast/Tox21 data were from *in vitro* high throughput screening assays from numerous vendors and platforms (CompTox Chemicals Dashboard | Home (epa.gov); accessed 7-2021). Notably, the metabolic pathways for CPF, CPFO and $^{\Delta 9}$THC activate similar nuclear receptors and elements (e.g. aryl hydrocarbon receptor: Ahr; constitutive androstane receptor: CAR; farnesoid-X-receptor: FXR; liver-X-receptor: LXR; peroxisome proliferator activated receptors: PPAR; pregnane-X-receptor element: PXRE; PXR; retinoid-X-receptor: RXR), CYPs (CYP1A2, 2B6, 3A4, 2C19; 3A7) and transferase (UGT1A1) (Huestis, 2005, Testai et al., 2010, Dinis-Oliveira, 2016).

Biomolecular interactions in the ToxCast/Tox21 assays were measured for several intended target families (e.g., esterase, CYP, transferase, etc.) and target enzymes or proteins (e.g., esterase: AChE; CYP: cytochrome P450 CYP1A1; transferase: UDP-glucuronosyltransferase UGT1A1, glutathione-s-transferase GSTA2 & M3, sulfotransferase SULTA). Assay results on the CompTox Dashboard had been filtered through 7 levels in the ToxCast Pipeline that included caution flagging on curve fitting (Level 6, indications of false positives) (Filer et al., 2017). Assays were downloaded from the CompTox Chemicals Dashboard (Supplemental Tables 1-3), then examined for active hit-calls, AC_{50} values, cytotoxicity limits (unique to each chemical), cautionary flags, and relevance to MOA/eCBS (Judson et al., 2016, Williams et al., 2017). The cytotoxicity limit occurs in a narrow range of concentrations coinciding with a sharp increase in active hit-calls (Judson et al., 2016). Within a region of 'cytotoxicity-associated burst,' leading up to the 'concentration threshold/limit,' the observed assay active hit-calls are potentially due to cell stress and cytotoxicity rather than compound-specific activity (Judson et al., 2016).[2]

3.4. High throughput toxicokinetics

The ICE 3COMP and PBTK oral models (https://ice.ntp.niehs.nih.gov/; version 3.5; accessed 1/2022; Bell et al. (2020a)), were tested for their ability to predict *in vivo* PODs by *in vitro* to *in vivo* extrapolation (IVIVE). The oral models were selected since this is the most likely exposure route based on the PODs selected from animal studies. The open access "httk" R Package (https://CRAN.R-project.org/package=httk; Breen et al. (2021)) in the ICE program (https://ice.ntp.niehs.nih.gov/; version 3.5; accessed 1/2022; Bell et al. (2020a) uses ToxCast/Tox21 AC_{50}s as the data inputs. The HTTK-based 3COMP and PBTK programs allow the incorporation of chemical-specific TK characteristics (e.g., metabolic properties) based on *in vitro* measurements and/or *in silico* predictions (Bessems et al., 2014). Visual depictions of and calculations for each model are detailed in Pearce et al. (2017). Toxicodynamic parameters (i.e., intraspecies extrapolations) are not integrated into the 3COMP, PBTK or HTTK-Pop$_{\text{Human}}$ models because they are reliant on dynamic chemical interactions at a target site to initiate a specific toxicologically significant response (e.g., estrogen receptor and endocrine disruption) (Choi et al., 2004). This is important to note because a given ToxCast/Tox21 assay may not have the metabolic capability or design to capture a representative *in vivo* toxicodynamic interaction.

The 3COMP oral model has perfusion rate-limited compartments (i.e., equilibrium is achieved rapidly for tissue, RBC and plasma compared to flow of blood) comprised of gut, liver, and rest-of-body (e.g., fat, brain, bones). The "Solve_3comp" model from the open access ICE tool calculates plasma concentration over time. Hepatic metabolism and passive glomerular filtration of chemicals is the assumed form of elimination (https://CRAN.R-project.org/package=httk; Wambaugh et al. (2015a); Breen et al. (2021)).

The "Solve_pbtk" multicompartment (gut, artery, vein, lung, liver, kidney, rest-of-body) function in the open access ICE tool calculates C_{max} for oral exposure at the 50th percentile using the average values for the PKTK parameters over time. Each compartment is perfusion rate-limited and has mass balance differential equations describing rate of change for quantity of chemical (https://CRAN.R-project.org/package=httk); Wambaugh et al. (2015a); Breen et al. (2021)); calculations in Supplemental Table 4).

Both the "Solve_3comp" and Solve_pbtk" models, used the C_{max} in reverse dosimetry calculations as follows:

$$EADHuman\left(\frac{mg}{kg}\Big/d\right) = AC_{50}(\mu M)x\left(1\frac{mg}{kg}\Big/d\ \div Cmax\frac{mg}{kg}\Big/d\right) \quad (3)$$

[2] The cytotoxicity limit is set by taking the median AC_{50} for all of the cytotoxicity assays for the chemical of interest and moving about a factor of 10 lower (3 standard deviations of the average spread of cytotoxicity assays calculated across all chemicals). If an assay is below the cytotoxicity limit, it will most likely be below where cytotoxicity is seen for any cytotoxicity assay for that chemical. Therefore, most cytotoxicity assay AC_{50} values will be above the cytotoxicity limit (Personal Communication: Richard Judson, PhD, US EPA National Center for Computational Toxicology.

3.5. Population-based high throughput toxicokinetics

The HTTK-Pop method simulates human physiological variability by Monte Carlo sampling of the model parameters (e.g., liver flow, glomerular filtration rate, liver volume, concentration at steady state [C_{ss}], hepatic clearance, plasma protein binding) and reverse dosimetry to predict a human EAD (mg/kg/day) (Ring et al., 2017). Refinements incorporated by use of TK can decrease EAD $_{Human}$ variability by approximately 12% when compared to simpler *in vitro* to *in vivo* extrapolation models (Ring et al., 2017, Ring et al., 2021). The methods of deriving age-specific physiological parameters (e.g., hepatocellularity and liver mass) in the TK model "httk-pop" package have been detailed in Ring et al. (2017). The HTTK-Pop model uses regression equations from literature (McNally et al., 2014) and the biometrics of actual individuals (e.g., body weight) obtained from the National Health and Nutrition Examination Survey (NHANES; NHANES – National Health and Nutrition Examination Survey Homepage (cdc.gov); accessed 8/2021) to predict the age-specific physiological parameters employed in the TK models. However, the age-adjusted refinements were not designed to model all pharmacokinetic/pharmacodynamic parameters that might occur during development.

The initial R computer codes for HTTK-Pop EAD_{Human} were kindly provided by Dr. John Wambaugh, PhD, US EPA and then modified for this study (described in Supplemental Materials 1). To facilitate the computation of age-specific HTTK-EAD_{Human} values for each of the ToxCast/Tox21 assays, the R codes were modified to incorporate *in silico* data (Sipes et al., 2017) into the built-in HTTK TK data set as well as to utilize the two TK models available in the httk package: 3COMP and PBTK models. Predictions are programmed to occur based on age (0–80) at 5-year intervals (adjusted for liver to body weight) (Ring et al., 2017, Tan et al., 2007, Breen et al., 2021). The HTTK-Pop EAD $_{Human}$ in young children is predicted to be higher than adults due to a higher clearance per kilogram body weight at ages 2–10 (Ginsberg et al., 2002, Ginsberg et al., 2004). Metabolic enzyme ontogeny and physiology in that age range contribute to the increased clearance. Isozyme levels and activities are shown to be close to adult levels by 1 year of age such that the intrinsic clearance rate in children is equal to that of adults (Ginsberg et al., 2004). In addition, children have larger livers and greater blood flow per kilogram body weight than adults. The approximate human age equivalent of rat treatment was 0–4 years, and this was the selected age range used to generate the HTTK-Pop EAD_{Human}.

3.6. Evaluation of oral HTTK-Pop EAD $_{Human}$ Predictions

Predictability of HTTK-Pop EAD_{Human} values were examined by several steps:

1) Virtual population generator for HTTKpackage (HTTK-Pop) was used to derive HTTK-Pop EAD $_{Human}$ values for ages 0–4 using the MOA-related ToxCast/Tox21 AC_{50}s. Specifically, the 3COMP and PBTK models available within the httk package (Wambaugh et al., 2021) were run for each selected ToxCast/Tox21 assay with components/targets (e.g., esterase: AChE; CYP: CYP1A1; transferase: UGT1A1) related to the known MOAs and the eCBS.

2) The fold differences were determined between HTTK-Pop EAD $_{Human}$ (derived either from 3COMP or PBTK) and adjusted AS-ELOEL/LOELs (Nair and Jacob, 2016) or default UF-ELOEL/LOELs (WHO, 2017)). These fold differences were used to access the predictivity of different model-adjustment factor combinations: 3COMP:AS-ELOEL/LOEL, 3COMP:UF-ELOEL/LOEL, PBTK: AS-ELOEL/LOEL, and PBTK: UF-ELOEL/LOEL. Because all PK parameters are "human," (Pearce et al., 2017), the fold-differences between predicted (HTTK-Pop EAD $_{Human}$) and the adjusted ELOEL/LOELs can potentially be attributed to individual variability. All the fold differences from various model-scaling factor combinations were visualized using the method described in Pallmann and Hothorn (2016).

3) After selecting a suitable model-scaling factor combination, as a further measure of predictability, for each compound, a ToxCast/Tox21 assay with an active hit-call, but unrelated to the MOA, was selected (ATG_Oct_MLP_CIS_up, TOX21_DT40, and TOX21_DT40 for CPF, CPFO, and $^{\Delta 9}$THC, respectively; Supplemental Table 5). Each unrelated assay had one or fewer cautionary flags and a high AC_{50}, beyond the cytotoxicity limit, indicating borderline activity. HTTK-Pop EAD $_{Human}$ were calculated for these AC_{50}s and fold-differences between those and HTTK-Pop EAD $_{Human}$ related to the MOA were determined (i.e., "MOA Cut-off"). If the MOA-related fold-difference was less than the unrelated fold difference, then the HTTK-Pop EAD $_{Human}$ results could be considered predictive to the chemical's MOA. All the fold differences were presented graphically using the method by Pallmann and Hothorn (2016).

HTTK-Pop EAD $_{Human}$ for each compound were calculated and the most predictive PODs were based on:

- Fold-differences with *in vivo* POD
- Fold differences between Predicted EAD_{Human} POD from assays unrelated to the MOAs compared to predicted EAD_{Human} from MOA targets (Supplemental Table 7).

4. Results

4.1. Open access literature: in vivo study selections

In vivo targets involved with metabolic activation that are common among CPF, CPFO and $^{\Delta 9}$THC were the focus of comparisons with the *in vitro*/computational mechanistic predictions. Targets related to the eCBS, also common among the 3 chemicals, was of interest since this is an area not previously studied by use of CompTox tools. Since there were no regulatory LOELs based on eCBS effects, they were estimated from available open literature. *In vivo* studies were performed using technical grade CPF, CPFO and $^{\Delta 9}$THC, standard strains of rat (Sprague-Dawley or Wistar), and treatments occurring within a similar age-range during early development (pre-weaning) to adolescence (Carr et al., 2020, Cha et al., 2006, Dow-Edwards and Zhao, 2008, Mohammed et al., 2018, O'Shea and Mallet, 2005, US EPA, 2011, Trezza et al., 2008). The MOA target activities are known to change (i.e., enzymes, nuclear receptors, etc.), depending on the developmental stage (Fernandez et al., 2011, Sadler et al., 2016, Tamási et al., 2003, Vyhlidal et al., 2006, Badée et al., 2019). Therefore, the relevance of the ToxCast/Tox21 assay targets for each chemical MOA is dependent on their activities during the developmental stage at treatment converted to human age (Table 1; Sengupta (2013): 1 human year = Rat days 26.7 (pre-weaning), 8.6 (weaning), 110.5 (pre-pubertal) and 34.8 (adult).

4.1.1. Chlorpyrifos

CPF directly affects the eCBS by significantly inhibiting FAAH resulting in an increase in AEA at a LOEL of 0.5 mg/kg/day in preweaning rat pups (Carr et al., 2020, Carr et al., 2017). Male and female Sprague-Dawley rat pups were treated by gavage (corn oil vehicle) post-natal days (PND) 10–16, (Human equivalent age: 0.73–1.17 years) (Carr et al., 2017, Sengupta, 2013). The time frame in rodents corresponds to a period of rapid human brain maturation involving increased myelination, synaptogenesis, and apoptosis (Tau and Peterson, 2010). It also corresponds to a developmental period when children may experience exposures to CPF through agricultural spray drift or hand-to-mouth soil ingestion from treated turf (CDPR, 2018), through contaminated $^{\Delta 9}$THC *in utero* or as second hand smoke/vaping. FAAH decreases and AEA increases were accompanied by behavioral effects at doses below the threshold for AChE inhibition

in rat brain (~1.0 mg/kg/day). Based on these data, 0.5 mg/kg/day was selected as the eCBS LOEL for CPF (Table 1).

4.1.2. Chlorpyrifos-oxon

Although CPF generally requires metabolic activation to form CPFO, in chlorine-treated drinking water, 100% converts to CPFO (US EPA, 2020a). Drinking water was a regulatory concern for the US EPA in their CPF human health risk assessment, especially for children and adolescents. Medina-Cleghorn et al. (2014) and Nomura et al. (2008) compared CPFO doses affecting the eCBS versus AChE inhibition in brain after intraperitoneal (i.p.) *in vivo* treatment. In each study, the effects on MAGL were approximately 3-fold lower than CPFO inhibition of brain AChE. CPFO brain AChE inhibition in post-natal day (PND) 11 (Human equivalent age: 0.8 years) Sprague-Dawley rats achieved a Benchmark Dose (BMD; BMR 10%) of 1.06 mg/kg/day. An uncertainty factor (UF) of 3 was used to extrapolate from brain AChE inhibition BMD_{10} (1.06 mg/kg/day) to the 3-fold lower effects on eCBS (FAAH and MAGL) inhibition (BMD_{10}: 1.06 mg/kg/day ÷ 3 = Estimated LOEL [ELOEL] 0.35 mg/kg/day) (Table 1). While this value is not an exact measurement of eCBS effects from CPFO treatment, it provides a reasonable estimation.

4.1.3. $^{\Delta 9}$Tetrahydrocannabinol

$^{\Delta 9}$THC developmental studies were available over a range of ages that covered the same preweaning test age as CPF and CPFO. These studies all resulted in behavioral effects that occurred at the same LOELs. For example, Wistar dams treated by gavage GD 15-PND 9 at 2.5 or 5.0 mg/kg/day (human equivalent age: GD 49–0.66 years; Sengupta (2013)) had pups with increased ultrasonic vocalizations at PND 12-day at 5.0 mg/kg/day. At PND 35 the pups had inhibited social interaction and anxiety at 5.0 mg/kg/day (Trezza et al., 2008). O'Shea and Mallet (2005) treated Wistar male rat pups PND 4–14 (human equivalent age: 0.29–1.02 years) with $^{\Delta 9}$THC at 5.0 mg/kg/day (intraperitoneal: i.p.) resulting in a decrease in percent correct choices in the delayed alternation test. Dow-Edwards and Zhao (2008) treated weanling Sprague-Dawley pups by gavage with $^{\Delta 9}$THC PND 22–40 (human equivalent age: 1.61–2.93 years) at 1.0 and 5.0 mg/kg/day. Locomotor activity and active avoidance were decreased at 5.0 mg/kg/day. Further, Cha et al. (2006) treated male adolescent Sprague-Dawley rats (PND 30; human equivalent age: 2.19 years) i.p. injection at 2.5, 5.0 and 10 mg/kg resulting in cognitive decrements in cognition at 5.0 mg/kg $^{\Delta 9}$THC. Reports have documented effects from human exposure to $^{\Delta 9}$THC at each of the above developmental stages resulting in long-term behavioral effects (Fried and Smith, 2001, Rubino et al., 2009). Therefore, within the age range of gestational to adolescent exposures, 5.0 mg/kg/day was selected as the LOEL for $^{\Delta 9}$THC during development (Table 1). Effects from $^{\Delta 9}$THC were assumed to be due to the eCBS disruption.

4.2. ToxCast/Tox21 active Hit-Calls

The number of active hit-calls for each chemical on the CompTox Chemicals Dashboard indicated the comparative toxicity (High CPFO > CPF > $^{\Delta 9}$THC Low) as tested by 14 vendors (CompTox Chemicals Dashboard | Home (epa.gov); accessed 8/2021) (Williams et al., 2017). The cytotoxicity limit for each compound, however, affects the number of active hit-calls that are potentially true actives based on AC_{50}s below the cytotoxicity limit (CPFO: 11.72 μM; CPF: 15.74 μM; $^{\Delta 9}$THC: 6.77 μM; Further description is presented in Judson et al. (2016)). In addition, the number of assays performed for CPF (854) and CPFO (978) was much greater than the number tested with $^{\Delta 9}$THC (79), indicating that the targeted assays for $^{\Delta 9}$THC/eCBS pathways may not currently be available. Table 2 presents a summary of 1) the critical components of the eCBS, CPF/CPFO and $^{\Delta 9}$THC pathways; 2) whether those components had assays in ToxCast/Tox21; 3) if so, how many were tested and of those, how many were active for each chemical and, 4) references associated with the pathway component. This summary provides a clearer overview of the specific assays with key components in the metabolic pathways for each chemical. There is some overlap in nuclear receptors and CYPS among the chemicals but the eCBS pathway is notably missing tests for essential targets (e.g., CBRs, FAAH, MAGL, adenylyl cyclase: ADYC, N-acyl-phosphatidylethanolamine phospholipase D: NAPE-DL, diacylglycerol lipase: DAGL, and others listed in Table 2) (Ahn et al., 2008, Benard et al., 2012, Berghuis et al., 2007, Berridge et al., 2010, Di Marzo et al., 2011, Djeungoue-Petga and Hebert-Chatelain, 2017, Fortin and Levine, 2007, Haj-Dahmane and Shen, 2010, Howlett et al., 2002, Iannotti and Vitale, 2021, Katona and Freund, 2012, Kirilly et al., 2013, Korpi et al., 2015, Pertwee et al., 2010, Snider et al., 2010, Viswakarma et al., 2010, Wang et al., 2003, Woods et al., 2007, Zendulka et al., 2016, Zou and Kumar, 2018). The lack of assays related to the eCBS indicated that it is currently not possible to test $^{\Delta 9}$THC with the critical parameters in the eCBS pathway.

Assays developed for various targets are determined by the vendors. Most of the active hit-calls had cautionary flags (potential false positives) reported as noisy (low signal-to-noise ratio), low efficacy (i.e., capacity of a drug to activate or inactivate a receptor), borderline active (only at highest concentration above baseline), or 'potentially confounded by overfitting the data'. Active hit-calls with cautionary flags were selected for 3COMP, PBTK and HTTK-Pop modeling given the following considerations: (1) Appearance of the dose–response curve; (2) relevance of the assay to the primary MOA, as well as presumptive secondary pathways associated with the eCBS; (3) an AC_{50} value greater than the lowest concentration screened (Friedman et al., 2019). Potential false positives, assays for viability parameters and/or not involved with the MOA or the eCBS were excluded from further analysis.

4.3. ToxCast/Tox21 targets and developmental age

While many target enzymes and proteins produced active hit-calls for each compound, the relevance of their activities was dependent on their age-related developmental stage. The nuclear receptors/elements (e.g. Ahr, CAR, FXR, LXR, PPAR, PXRE, PXR, RXR) associated with cytochrome P450 (CYP) regulation, are generally common to the metabolic pathways for CPF/CPFO and $^{\Delta 9}$THC, (Huestis, 2005, Testai et al., 2010, Dinis-Oliveira, 2016), but only CPF and CPFO had active hit-calls for these targets. Human neonatal activities for the nuclear receptors and CYPs may be 0–60% of adult values depending upon the CYP subfamily, inter- and intraindividual variability, assay test methods and available specimens (Allegaert and van den Anker, 2019, Sadler et al., 2016, Vyhlidal et al., 2006). Prenatal CYP3A7 is absent at birth and CYP1A1 achieves adult levels at 6–12 months. CYP1A2, 2B6, 3A4, 2C9 and 2C19 are steady throughout development and CYP3A4 increases postnatally. All reach adult levels at about 1–10 years of age (Ginsberg et al., 2002, Ginsberg et al., 2004). CPF/CPFO and $^{\Delta 9}$THC metabolism are primarily with CYP3A and 2C9 (Huestis, 2005, Testai et al., 2010, Dinis-Oliveira, 2016). The primary Phase II metabolic pathway with an active hit-call common to all three chemicals was glucuronidation by UGT1A1. Based on protein expression during development UGT1A1 reaches adult levels by 3–6 months (Badée et al., 2019). CPF and CPFO were active with glutathione-s-transferase (GSTA2) and CPFO was active with GSTM3 and sulfotransferase (SULT2A1) (Table 3). These Phase II enzymes reach adult levels in humans at approximately 2 weeks (GST) and >3 months (SULT2A1) (Hines, 2008). A dynamic balance between Phase I and Phase II metabolism determines the impact of chemical exposure on the developing fetus, child, and adolescent.

The eCBS is involved in the earliest stages of fetal brain development, including the GABAergic, glutamatergic, dopaminergic, and opioid receptor pathways (Fride, 2008, Wang et al., 2006). In relation to the eCBS, of the 129 G-protein coupled receptor (GPCR) assays on the

Table 1
In Vivo Endpoints for Chlorpyrifos, Chlorpyrifos-oxon and $^{\Delta 9}$Tetrahydrocannabinol.

Animal Strain	Rat Age Treated (Age Tested)	Approximate Human Years[a]	Effects	Measured Endpoints	Scaled Interspecies[b]	Default Interspecies[b]	Ref[c]
				mg/kg/day			
Chlorpyrifos							
Pup: Sprague-Dawley Rat M/F	Gavage PND 10–16	0.73–1.17 years	↓ FAAH & MAGL ↑Levels of AEA & 2-AG	LOEL 0.5	0.08	0.05	1
Chlorpyrifos-oxon							
Pup: Sprague-Dawley Rat M	Gavage PND 11	0.80 years	↓ Brain AChE activity	ELOEL 0.35[d]	0.057	0.035	2
Adult: Swiss-Webster Mice M	i.p. acute	NA	↓FAAH/MAGL activity				
$^{\Delta 9}$Tetrahydrocannabinol							
Dam: Wistar Rat Pup: M	Gavage GD 15-PND 9	GD 49–0.66 years	↓Activity ↑Stretch-attend postures & anxiety	LOEL 5.0	0.81	0.5	3
Neonatal Pup Wistar M	i.p. PND 4–14	0.29–1.02 years	↓ Cognition	LOEL 5.0 (only dose)	0.81	0.5	4
Weanling Rat Pup: Sprague-Dawley M/F	Gavage PND 22–40	0.52–12	↓Activity	LOEL 5.0	0.81	0.5	5
Adolescent Sprague-Dawley Rat M	i.p. PND 30	9.08	↓ Cognition	LOEL 5.0	0.81	0.5	6

Abbreviations: ELOEL: Estimated LOEL; F: Female; LOEL: Lowest-observed-effect-level; M: Male; PND: Postnatal Day.
Sengupta (2013): 1 human year = Rat days 26.7 (pre-weaning), 8.6 (weaning), 110.5 (pre-pubertal) and 34.8 (adult).
Lowest effect levels (ELOEL or LOEL) were scaled rat to human × 0.162 based on body weight or interspecies extrapolation was based on a default 10x uncertainty factor.
References: 1. Medina-Cleghorn et al. (2014), Nomura et al. (2008), US EPA (2011); 2. Carr et al. (2017), Buntyn et al. (2017), Carr et al. (2020); 3.Trezza et al. (2008); 4. O'Shea and Mallet (2005); 5. Dow-Edwards and Zhao (2008); 6. Cha et al. (2006).
CPFO inhibited MAGL in brain (Medina-Diaz et al., 2017, Nomura et al., 2008) at about 3-fold lower than brain AChE inhibition. An ELOEL = brain AChE inhibition Benchmark Dose (10% response) = 1.06 mg/kg/day in rat pups US EPA (2011) ÷ (3-fold uncertainty factor to extrapolate from AChE inhibition to FAAH/MAGL inhibition) = 0.35 mg/kg/day.

CompTox Chemicals Dashboard, none was for CB1 GPCR (activated by eCBs) and of the four available glutamate assays, none was active with CPF, CPFO or $^{\Delta 9}$THC. Assays with active hit-calls associated with the eCBS were for GABA, dopamine, and opioid receptors involved with neuronal pathways affected throughout brain development (Berghuis et al., 2007, Wang et al., 2006). Each of the neurotoxicity assays potentially associated with the eCBS was performed in the cell-free Novascreen (NVS) platform which measures effects of a chemical on a target protein, without whole-cell influences, such as metabolic activation.

4.4. ToxCast/Tox21 targets and Chlorpyrifos and Chlorpyrifos-Oxon

4.3.1. Metabolic pathway targets

The CPF MOA includes CPFO, and as the toxic metabolite, CPFO had more active hit-calls (Testai et al., 2010). Nuclear receptors/elements (i.e., CAR, LXR, PXRE, PXR; RXR, PPARɣ), CYPs (CYP1A2, 2B6, 3A4, 2C19; 3A7) and transferase (UGT1A1) and glutathione-s-transferase (GSTA2) target activities overlapped between CPF and CPFO, as might be expected (Table 3). The intended target families active with the CPFO metabolic pathway included nuclear receptors (PPAR, PXR, FXR, RXR and CAR) (Chang et al., 2003, Holick, 2005, Li et al., 2017, Michalik et al., 2006, Wang and Negishi, 2003, Chiu et al., 2021, Herriage et al., 2022, Viswakarma et al., 2010, Woods et al., 2007), CYPS (CYP2C19, CYP2B6, CYP1A2) (Foxenberg et al., 2011, Foxenberg et al., 2007, Mutch and Williams, 2006, Sams et al., 2000) and AChE (Testai et al., 2010). PXRE and PXR are associated with generalized liver metabolism and CYP induction (Wang and Negishi, 2003). The cell-free Novascreen assay for butyryl cholinesterase inhibition (NVS_ENZ_hES) had an active hit-call with CPF, although it is primarily inhibited by CPFO (Testai et al., 2010). Arylhydrolase receptor (Ahr) is associated with CYP1A2 in the CPF metabolic pathway (Foxenberg et al., 2007, Nebert et al., 2004). The lack of chemical specificity supports the evidence that CPF generally needs metabolic activation to the CPFO to achieve toxicity (Testai et al., 2010). Phase II GSTM3 and sulfotransferase (SULT2A1) were active with CPFO, along with UGT1A1 and GSH2A1, as mentioned previously (Medina-Díaz et al., 2011, Slotkin and Seidler, 2009, Testai et al., 2010).

4.3.2. Targets related to neurotoxicity or endocrine effects

The CPF active hit-call with the GABA receptor (NVS_LGIC_rGABAR_NonSelective) indicated a potential link to the eCBS which controls development of the GABAergic system (Berghuis et al., 2007). CPF affects GABA release through inhibition of FAAH in the eCBS (Berghuis, 2005, Carr et al., 2020, Pallotta et al., 2017). This cell-free assay was performed with extracted gene proteins from whole rat brain. An active hit-call was notable because the AC_{50} was below the CPF cytotoxicity limit (15.74 μM) and there were no cautionary flags (Table 3). However, of a total of 9 GABA receptor assays on the CompTox Dashboard, NVS_LGIC_rGABAR_NonSelective was the only one tested with CPF, therefore, it is difficult to draw a direct association of pathway perturbation based on a single result in a cell-free assay.

Neurodevelopmental toxicity involving dopamine was shown after CPF (hence, CPFO) treatment during development (Aldridge et al., 2005, Slotkin and Seidler, 2007). CB1 receptors interact with dopaminergic neurons affecting eCB production during early development (Berghuis et al., 2007). Although a dopamine target (DRD1: NVS_GPCR_hDRD1) AC_{50} was below the CPFO cytotoxicity limit (11.72 μM) (Table 3), it was the only active hit-call of 2 dopamine assays tested (of a total of 4 on the Dashboard). These results are insufficient to draw a direct association between dopamine as a CPF/CPFO target. However, *in vivo* an increase in N-methyl-D-aspartate receptor (NMDAR) subunits (NR1, NR2A and NR2B) at 0.1 mg/kg/day was reported in male rat pups treated with CPF in diet GD 7-PND 21 (Gomez-Gimenez et al., 2018). The NMDAR pathway in the hippocampus, activated by glutamine, leads to dopamine release in nucleus accumbens, affecting voluntary locomotor activity (Peleg-Raibstein and Feldon, 2006). When dopamine levels are depleted or when cells

Table 2
Components in the Endocannabinoid, CPF/CPFO and $^{\Delta 9}$-THC pathways in ToxCast/Tox21.

Components	Assays active/No. tested[a]			Assay Available in ToxCast/Tox21 (No. of assays)	References[b]
	CPF	CPFO	THC		
Endocannabinoid Pathway Components					**eCBS Pathway**
Opiate	X	2/2	X	Yes (5)	1, 2
PLC	--	--	--	No	3, 4
ADYC	X	X	X	Yes (3)	3, 5
DAGL	--	--	--	No	4, 6
NAPE-LD	--	--	--	No	4, 6
CB1R	--	--	--	No	3, 6
CB2R	--	--	--	No	3, 5
Mito CB1R	--	--	--	No	7, 8
MAP K	X	X	X	Yes (10)	1, 2
SIRT1	X	X	X	Yes (2)	9
miR22	--	--	--	No	9
p53	0/24	7/30	15/30	Yes (30)	9
GluNMDA	X	X	X	Yes (2)	3, 10
AMPA	X	X	X	Yes (1)	3, 11
DRD	0/4	1/1	X	Yes (11)	2, 12
5HT	0/1	X	X	Yes (6)	10, 13
GABAR	1/1	X	X	Yes (5)	3, 6, 10
GluR	X	X	X	Yes (2)	12, 13
SLC6A2	X	X	X	Yes (1)	10, 14
ACh	X	2/4	X	Yes (4)	5, 14
FAAH	--	--	--	No	4, 6
MAGL	--	--	--	No	4, 6
PPARα	0/2	0/2	X	Yes (2)	9
PPARγ	1/12	3/11	0/3	Yes (25)	1, 9
PPRE	0/2	1/2	X	Yes (2)	15, 16
PXRE	1/2	1/2	X	Yes (2)	15, 16
RXR	3/10	1/10	X	Yes (20)	15, 16
FXR	2/12	6/12	X	Yes (15)	16, 17
CAR	1/7	1/7	X	Yes (8)	16, 17
PXR	1/5	3/6	X	Yes (9)	16, 17
CYP2J2	X	X	X	Yes (2)	18, 19
CYP2C8	0/2	1/2	X	Yes (5)	18, 19
CYP2D6	X	X	X	Yes (2)	18, 19
CYP3A4	1/2	2/5	X	Yes (8)	18, 19
CYP2B6	1/2	5/7	X	Yes (8)	18, 19
CYP4X1	--	--	--	No	18, 19
CYP4F2	--	--	--	No	18, 19
CYP4A22	0/2	1/2	X	Yes (2)	18, 19
CYP4F3B	--	--	--	No	18, 19
Mito	2/7	4/19	X	Yes (22)	7, 8, 20
CPF/CPFO Metabolic Pathway					**CPF/CPFO Pathway**
PPARα	0/2	0/2	X	Yes (2)	21, 22
PPARγ	1/12	3/11	0/3	Yes (25)	21, 22
PPRE	0/2	1/2	X	Yes (2)	15, 16
PXRE	1/2	1/2	X	Yes (2)	15, 16
Ahr	2/4	0/4	1/2	Yes (4)	23, 24
RXR	3/10	1/10	X	Yes (20)	15, 16
FXR	2/12	6/12	X	Yes (15)	16, 17
CAR	1/7	1/7	X	Yes (8)	16, 17
PXR	1/5	3/6	X	Yes (9)	16, 17
CYP1A2	1/2	4/9	X	Yes (9)	25, 25, 27
CYP2B6	1/2	5/7	X	Yes (8)	25, 25, 27
CYP2C9	0/2	1/5	X	Yes (8)	25, 25, 27
CYP3A4	1/2	2/5	X	Yes (8)	25, 25, 27
CYP2C19	1/2	2/7	X	Yes (9)	25, 25, 27
CYP2D6	X	X	X	Yes (2)	25, 25, 27
CYP3A5	0/2	0/2	X	Yes (4)	25, 25, 27
PON1	--	--	--	No	25
AChE	X	2/4	X	Yes (4)	25
BuChE	1/2	1/2	X	Yes (2)	25
UGT	1/4	2/7	X	Yes (7)	25
SULTA	0/2	1/5	X	Yes (5)	25
GSH	1/4	2/7	X	Yes (7)	25, 28, 29
Mito	1/7	4/19	X	Yes (22)	7, 8. 20
$^{\Delta 9}$-THC Metabolic pathway					**$^{\Delta 9}$-THC References**
PPARα	0/2	0/2	X	Yes (2)	9
PPARγ	1/12	3/11	0/3	Yes (25)	1, 9
PPRE	0/2	1/2	X	Yes (2)	15, 16
PXRE	1/2	1/2	X	Yes (2)	15, 16
Ahr	2/4	0/4	1/2	Yes (4)	22, 23
RXR	3/10	1/10	X	Yes (20)	15, 16
FXR	2/12	6/12	X	Yes (15)	16, 17
CAR	1/7	1/7	X	Yes (8)	16, 17
PXR	1/5	3/6	X	Yes (9)	16, 17
CYP2C9	0/2	1/5	X	Yes (8)	9, 29
CYP2C19	1/2	2/7	X	Yes (9)	9, 29
CYP3A4	1/2	2/5	X	Yes (8)	9, 29
CYP1A1	1/2	3/9	X	Yes (9)	9
CYP1A2	1/2	4/9	X	Yes (9)	9
CYP1B1	X	X	X	Yes (2)	9
CYP2A6	X	X	X	Yes (3)	9
CYP2B6	1/2	5/7	X	Yes (8)	9
CYP2C9	0/2	1/5	X	Yes (8)	9
CYP2D6	X	X	X	Yes (2)	9
CYP3A5	0/2	0/2	X	Yes (4)	9
CYP3A7	1/2	1/2	X	Yes (2)	9
UGT	1/4	2/7	X	Yes (7)	9, 30
Mito	1/7	4/19	X	Yes (22)	7, 8, 20

a-"Yes" indicates there are assays in the CompTox Chemicals Dashboard and "No" indicates there are no assays (current as of the December 8, 2021: CompTox Chemicals Dashboard News (epa.gov); "()" indicates the number of assays available for testing. Note: Not all assays were tested for each chemical.

b- 1. Pertwee et al. (2010), 2. Berridge et al. (2010), 3. Korpi et al. (2015), 4. Di Marzo (2011), 5. Howlett et al. (2002), 6. Berghuis et al. (2007), 7. Benard et al. (2012), 8. Djeungoue-Petga and Hebert-Chatelain (2017), 9. Iannotti and Vitale (2021), 10. Kirilly et al. (2013), 11. Ahn et al. (2008), 12. Haj-Dahmane and Shen (2010), 13. Fortin and Levine (2007), 14. Katona and Freund (2012), 15. Viswakarma et al. (2010), 16. Wang and Negishi (2003), 17. Woods et al. (2007), 18. Zendulka et al. (2016), 19. Snider et al. (2010), 20. Zou and Kumar (2018), 21. Chiu et al. (2021), 22. Herriage et al. (2022), 23. Foxenberg et al. (2007), 24. Nebert et al. (2004), 25. Testai et al. (2010), 26. Sams et al. (2000), 27. Mutch and Williams (2006), 28. Medina-Díaz et al. (2011), 29. Slotkin and Seidler (2009), 30. Dinis-Oliveira (2016).
Abbreviations: ADYC: Adenyl cyclase; ACh/AChE: acetylcholine/esterase; Ahr: arylhydrocarbon hydroxylase receptor; AMPA: α-amino-3-hydroxy-5-methyl-4-isoxazolepropionic acid BuChE: butyryl cholinesterase; CAR: constitutive androstane receptor; CB1R/CB2R: cannabinoid receptors 1 & 2; CYP: p450 isozymes; DAGL: diaceylglycerol lipase; DRD: dopamine; FAAH: fatty acid amid hydrolase; GABAR: ɣ-amino butyric acid receptor; GluR: glutamate receptor; GSH: Glutathione-s-transferase; GPCR: G-coupled protein receptor; MAGL: monoacylglycerol lipase; MAPK: mitogen-activated protein kinase; miR22: micro RNA 22; Mito: mitochondria; Mito CB1R: mitochondrial CB1 receptor; NAPE-LD: N-acyl-phosphatidylethanolamine phospholipase D; NMDAR: N-methyl- D-aspartic acid receptor; NT: not tested by CPF/CPO or $^{\Delta 9}$-THC; p53: tumor protein 53; PLC: phospholipase C; PON1: paraoxonase 1: PPAR: peroxisome proliferator-activated receptor; PPRE: PXR: pregnane-x-receptor; PXRE: pregnane-x-receptor element; RXR: retinoid-x-receptor; SIRT1: NAD-dependent deacetylase sirtuin-1; SLC6A2: norepinephrine transporter; SULTA: sulfotransferase; UGT: UDP-glucuronosyltransferase.
Green boxes: ToxCast/Tox21 assays available and reported on CompTox Chemicals Dashboard (epa.gov) (December 8, 2021 version); Red boxes: no available tests on the CompTox Chemicals Dashboard; "—" = No ToxCast/Tox21 assay for this component; "**X**" = Chemical not tested in the assay.

cannot synthesize it, motor control in the cerebellum or other motor control areas of the CNS, cannot function normally.

The opioid receptor assays (NVS_GPCR_rOpiate_NonSelective, NVS_GPCR_rOpiate_NonSelectiveNa) performed with rat forebrain membrane proteins and CPFO had AC_{50}s of 12 μM (cusp of the cytotoxicity limit: 11.72 μM) and 21 μM, respectively (Table 3). *In vivo* activity at this receptor showed prenatal $^{\Delta 9}$THC treatment in rats resulted in changes in μ-opioid receptor binding and increased morphine and heroin self-administration in F1 females (Vela et al., 1998). Effects were also observed in opioid gene expression in human fetal brains associated with marijuana use in the mothers (Wang et al., 2006). Given the fact that CPF/CPFO disrupt the eCBS during development, there is potential for accompanying developmental effects on associated neurotransmitter systems (Alugubelly et al., 2021).

Mitochondria assays had active hit-calls with CPF and CPFO. Mitochondrial targets are of interest because CPF suppresses mitochondrial oxidative phosphorylation in dopaminergic neurons during development (Singh et al., 2018). CPF and CPFO decreased mitochondrial length, number, and transport in cultured cortical neurons of PND 1 Sprague-Dawley rats (Middlemore-Risher et al., 2011). These effects may occur through the mtCB1 receptor thus involving the eCBS. However, of the 25 ToxCast/Tox21 assays available, CPF (tested in 7 assays) had only a single active hit-call (NCCT_MITO_max_resp_rate_OCR_dn) and CPFO (tested in 13 assays) had only 2 active hit calls (NCCT_MITO_basal_resp_rate_OCR_dn, and NCCT_MITO_max_resp_rate_OCR_dn). The AC_{50}s were above the cytotoxicity limit, indicating only a weak interaction.

In judging whether the GABA, dopamine, opiate or mitochondrial pathways are active with CPF or CPFO based on ToxCast/Tox21 assay results, there are a few issues to consider: 1) the USEPA considers that a chemical should be active in at least 5 pathway-mapped assays to have a positive pathway association (Judson et al., 2010); 2) each of the CNS-associated assays was a NovaScreen cell-free assay, meaning

Table 3
Fold Difference between CPF, CPFO or $^{\Delta 9}$THC *In Vivo* and 3 Compartment or PBTK-Modeled Endpoints.

Target	ToxCast/Tox21 Assay[a]	AC_{50} (μM)[b]	Fold Difference in Oral HTTK Models				3COMP Oral EAD_{Human} (mg/kg/day)
			Allometric Scaling[c]		Default UF[c]		
			3COMP	PBTK	3COMP	PBTK	
Chlorpyrifos							
NR	ATG_**PXRE**_CIS_up	6	8	22	14	35	0.68
NR	ATG_**PXR**_TRANS_up	4	6	15	9	24	0.46
NR	OT_**FXR**_FXRSRC1_1440	44	59	152	95	246	4.74
NR	ATG_**PPARg**_TRANS_up	57	75	195	122	316	6.11
NR	TOX21_**CAR**_Agonist	40	52	136	85	220	4.24
NR	ATG_DR4_**LXR**_CIS_dn	35	46	120	75	195	3.76
DB	OT_NURR1_NURR1**RXRa**_0480	39	52	135	84	218	4.21
DB	ATG_**RXRb**_TRANS_up	24	32	82	51	133	2.57
DB	TOX21_**AhR**_LUC_Agonist	39	52	135	84	218	4.21
DB	ATG_**Ahr**_CIS_up	2	3	8	5	13	0.25
ES	NVS_**ENZ**_hES	29	38	98	61	158	3.05
CYP	LTEA_HepaRG_**CYP2B6**_up	14	18	48	30	77	1.50
CYP	NVS_ADME_**hCYP2B6**	34	45	117	73	190	3.66
CYP	LTEA_HepaRG_**CYP3A4**_up	31	40	104	65	169	3.27
CYP	LTEA_HepaRG_**CYP3A7**_up	50	66	172	108	279	5.38
TF	LTEA_HepaRG_**UGT1A**1_up	38	49	128	80	207	4.01
TF	LTEA_HepaRG_**GSTA2**_up	0.31	2.4	1	1	2	0.03
IC	NVS_LGIC_r**GABAR**_NonSelective	12	16	42	26	68	1.31
Mito	NCCT_**MITO**_max_resp_rate_OCR_dn	66	87	224	140	363	7.02
Chlorpyrifos-oxon							
NR	ATG_**PPRE**_CIS_up	33	221	275	358	445	13
NR	ATG_**PXRE**_CIS_up	43	290	360	469	583	16
NR	OT_**FXR**_FXRSRC1_1440	0.31	2	3	3	4	0.12
NR	TOX21_**FXR**_BLA_antagonist_ratio	17	115	143	186	231	6.5
NR	OT_NURR1_NURR1**RXRa**_1440	43	289	359	468	582	16
NR	ATG_**PPARg**_TRANS_up	34	231	287	374	465	13
NR	TOX21_**PPARg**_BLA_antagonist_ratio	1	7	9	12	15	0.42
NR	NVS_NR_**hCAR**_Antagonist	22	149	185	241	299	8.43
CYP	TOX21_**Aromatase_Inhibition**	24	161	200	261	324	9.12
CYP	NVS_ADME_**hCYP1A1**	8	58	72	93	116	3.27
CYP	CLD_**CYP1A1**_6hr	5	36	45	58	72	2.04
CYP	LTEA_HepaRG_**CYP1A1**_up	40	271	337	439	545	15
CYP	NVS_ADME_h**CYP1A2**	4	26	32	42	52	1.46
CYP	CLD_**CYP1A2**_24hr	3	23	29	38	47	1.32
CYP	NVS_ADME_h**CYP2C19**	4	28	34	45	56	1.57
CYP	CLD_**CYP2B6**_24hr	0.4	3	3	4	6	0.16
CYP	NVS_ADME_h**CYP2B6**	9	61	76	99	124	3.48
CYP	CLD_**CYP3A4**_6hr	12	81	100	131	163	4.58
ES	NVS_ENZ_r**AChE**	0.96	7	8	11	13	0.37
ES	NVS_ENZ_h**AChE**	0.32	2	3	4	4	0.12
TF	CLD_**UGT1A1**_48hr	5	31	39	50	62	1.76
TF	LTEA_HepaRG_**GSTA2**_dn	47.8	380	763	615	1236	21
TF	LTEA_HepaRG_**GSTM3**_dn	91.9	730	1467	1182	2376	41
TF	LTEA_HepaRG_**SULT2A1**_dn	75.0	596	1197	965	1939	34
GPCR	NVS_GPCR_h**DRD1**	8	56	70	91	114	3.2
GPCR	NVS_GPCR_**rOpiate_NonSelectiveNa**	21	142	176	230	286	8.04
GPCR	NVS_GPCR_**rOpiate**_NonSelective	12	81	101	132	164	4.62
Mito	NCCT_**MITO**_basal_resp_rate_OCR_dn	27	185	230	300	373	11
Mito	NCCT_**MITO**_max_resp_rate_OCR_dn	32	216	269	351	436	12
$^{\Delta 9}$Tetrahydrocannabinol							
CYP	TOX21_**Aromatase_Inhibition**	29	7	70	11	113	5.57
DB	TOX21_**AhR**_LUC_Agonist	18	4	42	7	68	3.34
DB	TOX21_**p53**_BLA_p1_ratio	32	8	76	12	124	6.12
DB	TOX21_**p53**_BLA_p2_ratio	33	8	78	13	127	6.28
DB	TOX21_**p53**_BLA_p3_ratio	34	8	81	13	132	6.52
DB	TOX21_**p53**_BLA_p4_ratio	33	8	78	12	126	6.22
DB	TOX21_**p53**_BLA_p5_ratio	41	10	97	16	158	7.80
NR	TOX21_**AR**_LUC_MDAKB2_Antagonist_10nM_R1881	43	10	102	16	165	8.17
NR	TOX21_**AR**_BLA_Antagonist_ratio	7.6	2	18	3	29	1.45
NR	TOX21_**ERa**_BLA_Antagonist_ratio	56	13	133	21	216	11
NR	TOX21_**ERa**_LUC_VM7_Antagonist_0.5nM_E2	11	3	27	4	44	2.16
NR	TOX21_**GR**_BLA_Agonist_ratio	35	8	82	13	133	6.58
NR	TOX21_**TR**_LUC_GH3_Antagonist	14	3	32	5	52	2.59

Abbreviations: CYP: Cytochrome P450; DB: DNA binding; EAD_{Human}: Equivalent Administered Dose (human); ES: Esterase; GPCR: G-Protein coupled receptor; IC: Ion Channel; Mito: Mitochondria; NR: Nuclear Receptor; PBTK: Physiologically Based Toxicokinetic model; TF: Transferase; UF: Uncertainty Factor.
a- **Bold** text in the assay description indicates target enzyme, protein, or receptor of interest.

b- **Bolded Red** AC_{50} values are below the cytotoxicity limits: CPF = 15.74 μM; CPFO = 11.72 μM; $^{\Delta 9}$THC = 6.77 μM.
c- Fold-difference between the predicted EAD_{Human} (mg/kg/day) and the *in vivo* scaled LOEL (CPF = 0.081 & $^{\Delta 9}$THC = 0.81 mg/kg/day) or scaled ELOEL (CPFO = 0.057 mg/kg/day) or default interspecies 10x UF LOEL (CPF = 0.05 & $^{\Delta 9}$THC = 0.5 mg/kg/day) or UF ELOEL (CPFO = 0.035 mg/kg/day) rounded to the nearest two digits. Green: ≤10-fold difference; Yellow: >10 ≤ 100-fold difference and Red: >100-fold-difference.

that they were ligand binding in the absence of cellular effects and 3) there were no assays for many of the eCBS components listed in Table 3 available that could support an association between these active hit-calls and targeted eCBS effects. While there is a link between CPF/CPFO and eCBS pathways affecting dopamine, GABA and opiate receptors in the brain (Aldridge et al., 2005, Eaton et al., 2008, Leung et al., 2019, Alugubelly et al., 2021, Slotkin and Seidler, 2010), the data from ToxCast/Tox21 do not directly support an association of either chemical with these pathways.

Although there were active hit-calls with the estrogen (ER), progesterone (PR), androgen (AR), thyroid (TR) and steroid hormone targets, based on the weight-of-evidence, CPF and CPFO are not considered to be endocrine disruptors (https://www.epa.gov/endocrine-disruption/endocrine-disruptor-screening-program-tier-1-screening-determinations-and; accessed 8-2021). The active hit-call aromatase inhibition assay (TOX21_Aromatase_Inhibition) relates to CYP19A1, which is involved with estrogen bioactivity (CYP19A1 cytochrome P450 family 19 subfamily A member 1 [Homo sapiens (human)] - Gene - NCBI (nih.gov); accessed 1-2021) but not CPFO metabolism.

4.5. ToxCast/Tox21 targets and $^{\Delta 9}$Tetrahydrocannabinol

$^{\Delta 9}$THC was active with the nuclear receptor Ahr (TOX21_AhR_LUC_Agonist) which is associated with CYP1A2 in the MOA (Huestis, 2005, Dinis-Oliveira, 2016) (Table 3). The only CYP activity was with aromatase inhibition (TOX21_Aromatase_Inhibition) which is associated with estrogenic bioactivity through expression of CYP19A1 (CYP19A1 cytochrome P450 family 19 subfamily A member 1 [Homo sapiens (human)] - Gene - NCBI (nih.gov); accessed 1-2021). $^{\Delta 9}$THC had active hit-calls for AR, ER, TR, and GR assays which may relate to the adverse *in vivo* effects $^{\Delta 9}$THC was shown to have on human sperm and on the fertilization process in male and female reproductive tracts (Table 3) (Lee et al., 2020, Payne et al., 2019). However, because the AC_{50}s were above the cytotoxicity limit, a target specific $^{\Delta 9}$THC interaction cannot be determined.

There were overall differences in the ToxCast/Tox21 assays tested with $^{\Delta 9}$THC, compared to CPF/CPFO. For example, only 79 assays were performed with $^{\Delta 9}$THC because this chemical was only tested in the National Institutes of Health National Center for Advancing Translational Sciences (NIH NCATS) using their assays (Tox21 National Institutes of Health Chemical Genomics Center: NCGC). CPF/CPFO active assays were performed by numerous vendors supported by the US EPA, NIH NCATS and the NIH National Toxicology Program (Table 3; Supplemental Tables 1-3; vendor data available through: CompTox Chemicals Dashboard | Home (epa.gov)).

The Tox21 (NCGC) active hit-calls with $^{\Delta 9}$THC were mainly cytotoxicity, cell stress or cell-stress-related interference assays and not likely to have specific biological significance (20/34; Supplemental Table 3). Cytotoxicity is a very high concentration effect and not target specific toxicity which is usually driven by more specific mechanisms at lower doses (R. Judson, PhD, USEPA, personal communication). The 14 assays that were not designed to assess cytotoxicity had no AC_{50}s below the cytotoxicity limit. But this is primarily due to not having the right assays to characterize $^{\Delta 9}$THC activity. For example, had biologically significant assays for CB1 receptors been available, a $^{\Delta 9}$THC active hit-call would have likely been active below the cytotoxicity limit. Moreover, cytotoxicity varies depending on the metabolic capability of different cell types, their growth rates and toxicokinetics associated with toxic effects from a given chemical (Judge et al., 2016). Since there was no metabolic activation employed in the ToxCast/Tox21 assays (unless the cells possess intrinsic metabolic activation capability), the formation of active metabolites is unlikely. In the absence of assays with biological activity specific to $^{\Delta 9}$THC, such as a CB1 receptor assay, the available ToxCast/Tox21 assays may be unable to provide useful information on the key steps in elucidating MOA for $^{\Delta 9}$THC.

4.4. HTTK 3COMP and PBTK modeled predictions compared to in vivo scaled or default Interspecies-Adjusted ELOEL or LOEL points of departure

4.4.1. Qualitative evaluation

Fig. 1 shows the comparison between *in vivo* PODs derived from experimental animal studies and model predictions (i.e., EAD_{Human}) using IVIVE tools available in the HTTK package (i.e., 3COMP and PBTK oral models). Natural logarithm values (ln) were used in presenting the values because of the broad variation in the fold differences (Table 3). The HTTK 3COMP and PBTK oral models predicted the EAD_{Human} for each chemical using ToxCast/Tox21 assay AC_{50} data as model inputs (https://CRAN.R-project.org/package=httk); Wambaugh et al. (2015a); Breen et al. (2021)) with the intraspecies (i.e., human) variability being generated by Monte Carlo distributions as described in Pearce et al (2017). Prior to the comparison, the *in vivo* PODs were converted into "human equivalent values" by using either allometric scaling factor (AS) (Nair and Jacob, 2016) or traditional interspecies uncertainty factor (UF). Instead of further adjusting the "human equivalent values," two horizontal lines are used to represent the distance from "perfect match" (i.e., ln(1) = 0) to "maximum uncertainty" (i.e., ln(10) = 2.3) due to intraspecies (human) variation between the *in vivo*- and HTTK model-based values. As can be seen in Fig. 1, PBTK model predicted EAD_{Human} values exhibited distances further away from both the line = 0 and line = 2.3 ("blue cluster") than 3COMP model ("pink cluster"), and allometric scaling (AS) provided a lesser fold difference than traditional UF regardless of the HTTK models employed. For risk assessment, log fold-differences at or below the cut-off (i.e., closer to log fold-difference = 0) represent ToxCast/Tox21 target assays that are likely the most relevant to the MOA/eCBS. Accordingly, the 3COMP model and allometric scaling were used in the subsequent analyses for identifying the most relevant MOA/eCBS.

Table 3 shows no $^{\Delta 9}$THC AC_{50}s below the cytotoxicity limit (6.77 μM). While the fold differences were predictive for this compound with the 3COMP model and AS-LOEL, they were not meaningful because the AC_{50}s exceeded the cytotoxicity range. Therefore, further qualitative data refinement for $^{\Delta 9}$THC was not performed. For CPF and CPFO, the 3COMP model with AS interspecies extrapolation generated EAD_{Human} values that were more predictive than the PBTK model by AS or UF interspecies extrapolation. Fig. 2 provides a closer inspection of the distributions of ln fold-differences between the *in vivo* AS-ELOEL/LOELs and EAD_{Human} values for CPF and CPFO. The dotted lines (i.e., "MOA Cut-Off") in Fig. 2 approximates the ln fold-differences between the *in vivo* AS-ELOEL/LOEL and the ToxCast/Tox21 assays that are not related to the MOA/eCBS. Fold-difference above this line shows ToxCast/Tox21 assay activity that is not likely specific to the MOA/eCBS for each chemical and below the EAD_{Human} values are predictive.

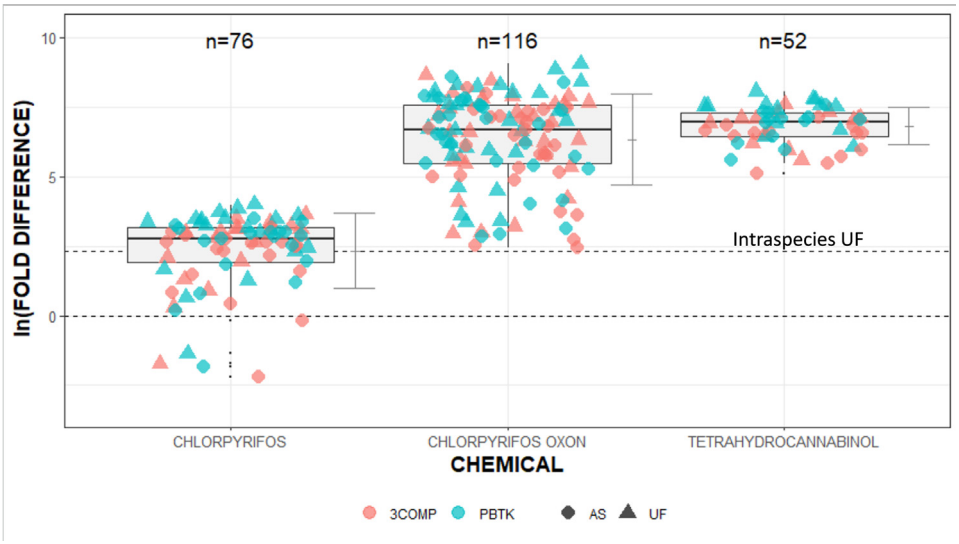

Fig. 1. Natural logarithm fold-differences between 3COMP or PBTK models EAD_{Human} and *in vivo* PODs determined by allometric scaling (AS) or default 10-fold uncertainty factor (UF). The dotted lines describe the "perfect match" (ln(1) = 0) and "maximum uncertainty" (ln(10) = 2.3) due to intraspecies (human) variation between the *in vivo*- and httk model-based values. The vertical bars are the standard deviation of fold-differences.

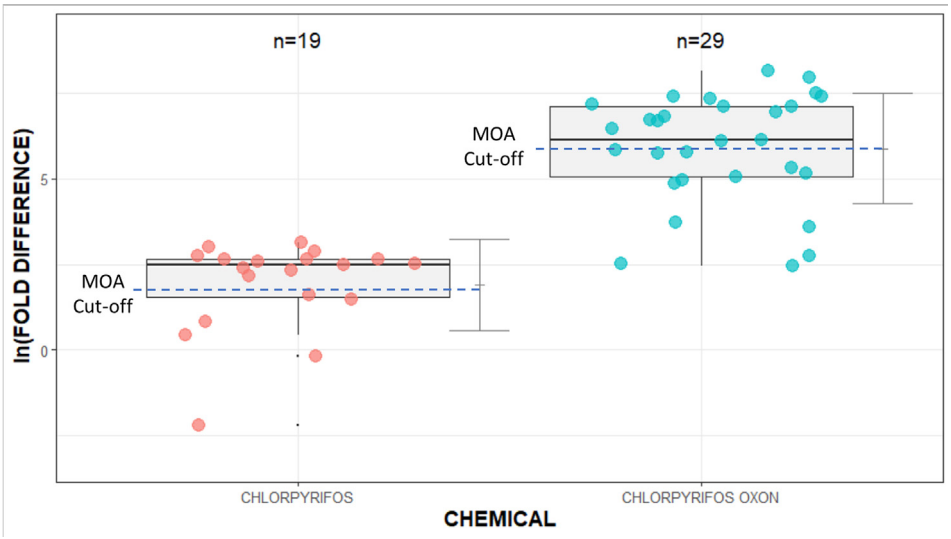

Fig. 2. CPF and CPFO natural logarithm fold-differences between the EAD_{Human} with the 3COMP model and *in vivo* PODs with AS interspecies extrapolation. The dotted lines approximate the natural logarithm fold-difference between the *in vivo* AS-ELOEL/LOEL and the ToxCast/Tox21 assays that are not related to the MOA/eCBS. Assays below the lines for the respective chemicals are likely to be associated with the MOA/eCBS.

4.4.2. Quantitative evaluation

Assays (AC_{50}s) for model inputs were selected for potential relevance to MOA/eCBS (Table 3). The lower AC_{50} value was used when identical ToxCast/Tox21 assays showed active hit-calls for different durations. For example, the CPFO AC_{50} for CYP2B6 at 24 h was 0.404 μM but at 48 h it was 11.2 μM so the result at 24 h was a more sensitive interval for that assay. The heat maps in Table 3 provide a qualitative visualization and quantitative fold-differences between *in vivo* AS or UF interspecies extrapolation and EAD_{Human} predictions. Quantitatively, both 3COMP and PBTK models have lower the fold-differences using the AS with ELOEL/LOEL PODs than for UF interspecies extrapolation. Further the 3COMP model is quantitatively more predictive for all compounds than the PBTK model (Table 3; Calculations in Supplemental Table 4). The 3COMP/EAD_{Human} CPF and $^{\Delta 9}$THC values were more predictive of *in vivo* AS-adjusted PODs than those of CPFO, where quantitative ranking of the fold difference calculations was categorized as: 1) **Green:** Fold differences within one order of magnitude of the *in vivo* scaled ELOEL or LOEL (≤10-fold); 2) **Yellow:** Fold differences within 1–2 orders of magnitude (>10 ≤ 100-fold) and 3) **Red:** Fold differences > 100-fold.

In Table 3, fold differences indicated that the EAD_{Human} were more predictive for $^{\Delta 9}$THC than for CPF or CPFO. However, fold differences in relation to model predictability need to be interpreted with caution because several factors influence the outcomes. For example, an assay with an active hit-call, must be screened for cautionary flags, should be relevant to a mechanistic pathway, have an acceptable dose–response curve, and have an AC_{50} below the cytotoxicity limit to indicate a degree of chemical-target specificity. The CPF LTEA_HepaRG_GSTA2_up assay had most of the criteria, and few cautionary flags, but the dose–response curve was visually not acceptable. Therefore, this assay was not included for further analysis in HTTK-Pop. $^{\Delta 9}$THC had no AC_{50}s below the cytotoxicity limit. Even though the fold differ-

ences appeared predictive, they were not because the ToxCast/Tox21 AC_{50}s were primarily cytotoxic, and the assays were unrelated to specific biological activity in the known metabolic pathway (Table 2).

4.5. 3 COMP HTTK-Pop EAD $_{human}$ predictions compared to in vivo allometrically scaled points of departure

The ToxCast/Tox21 assays in Table 4 were selected by the following criteria: 1) targets were relevant to the MOA/eCBS; 2) AC_{50}s were at or below the cytotoxicity limit; 2) fold-differences were within a predictive (CPF: 1–5 fold) or moderately predictive (CPFO: 12–41 fold) range; 3) had fold-differences below those of the "Unrelated" HTTK-Pop (age 0–4) values delineating an upper bound of activity; and 4) had acceptable dose–response curves. Many of the assays were for nuclear receptors (PXRE/PXR/Ahr/FXR/PPARg), although both CPF and CPFO were active with CYP2B6 as could be expected (Testai et al., 2010). CPF was active with a GABA receptor, however, this association would be downstream from CPF inhibition of FAAH (Carr et al., 2017) and subsequent inhibition of presynaptic GABA release (Leung et al., 2019). CPFO was also active with AChE which is a direct target for the MOA. $^{\Delta 9}$THC results were not included because none of the selection criteria were met (data in Supplemental Tables 6,7).

4.6. Concordance between in vivo data and predictions from CompTox tools

The results of the stepwise process of gathering *in vivo* and *in vitro* data, selecting ToxCast/Tox21 data relevant to the known MOA/eCBS pathways, determining the most predictive HTTK model and interspecies extrapolation method and refining the predictions based on age by use of HTTK-Pop Data are summarized in Table 5. ToxCast/Tox21 results indicated a weak link between CPF and CPFO and GABA, dopamine, opioid and mitochondrial targets that are known to be affected by CPF treatment and associated with the eCBS (Berghuis, 2005, Berghuis et al., 2007, Fernández-Ruiz et al., 2019, Navarro et al., 1996, Fernández-Ruiz et al., 2004, Bénard et al., 2012, Djeungoue-Petga and Hebert-Chatelain, 2017, Fride, 2004, Wang et al., 2006). However, the ToxCast/Tox21 results alone would not have supported an association. Endocrine assays for $^{\Delta 9}$THC resulted in high AC_{50}s and did not offer a strong support for a specific chemical-related association although an association has been shown *in vivo* (Lee et al., 2020, Payne et al., 2019). The AS 3COMP model was more predictive than the AS PBTK, and both models indicated there was very likely a need for metabolic activation of CPF to CPFO to identify biological targets. $^{\Delta 9}$THC EAD_{Human} was predictive but the predictions were not biologically meaningful because the ToxCast/Tox21 targets were not specific to the metabolic pathway.

Table 4
ToxCast/Tox21 Assays in the 3COMP HTTK-Pop Model with Associated Fold Differences Measured Against Upper Bound Controls and Allometric Scaled ELOEL/LOELs for CPF and CPFO.

Target	AC_{50} (μM)	3C Oral EAD_{Human} (mg/kg/day) Age 0–4	Fold-Difference[a] EAD_{Human}:AS-ELOEL/LOEL	UR Reference AC_{50} (uM)	UR EAD_{Human} (mg/kg/d) Age 0–4	Fold Difference[a] UR-EAD_{Human}:AS-ELOEL/LOEL
Chlorpyrifos						
ATG_PXRE_CIS_up	6.34	0.182	2	110	3.17	6.33
ATG_PXR_TRANS_up	4.34	0.125	2	110	3.17	6.33
ATG_Ahr_CIS_up	2.35	0.068	1	110	3.17	6.33
LTEA_HepARG_CYP2B6_up	14	0.403	5	110	3.17	6.33
NVS_LGIC_rGABAR_NonSelective	12	0.354	4	110	3.17	6.33
Chlorpyrifos-oxon						
OT_FXR_FXRSRC1_1440	0.307	0.66	12	80.1	173	493
TOX21_PPARg_BLA_antagonist_ratio	1.08	2.33	41	80.1	173	493
CLD_CYP2B6_24hr	0.404	0.87	15	80.1	173	493
NVS_ENZ_hAChE	0.323	0.70	12	80.1	173	493

Abbreviations: AS-ELOEL/LOEL: Allometrically scaled *in vivo* PODs (CPF 0.081 and CPFO 0.057 mg/kg/day); 3C: 3 Compartment Model; EAD_{Human}: Equivalent Administered Dose (human); UR: Assay unrelated to the CPF (ATG_Oct_MLP_CIS_up) and CPFO (TOX21_DT40); Supplemental Table 3.
a- Fold-difference between the HTTK-Pop predicted EAD_{Human} (mg/kg/day; ages 0–4) and the *in vivo* AS ELOEL/LOEL.

Table 5
Summary Data Relating to Computational Tools and Concordance of Predictions.

Parameter Measured	*Chlorpyrifos*		*Chlorpyrifos-oxon*		*$^{\Delta 9}$Tetrahydrocannabinol*	
In Vivo Points of Departure[a]	AS-LOEL: 0.08 mg/kg/day		AS-ELOEL: 0.057 mg/kg/day		AS-LOEL: 0.8 mg/kg/day	
ToxCast/Tox21 Assays[b]	Active Hit-Call Associations		Active Hit-Call Associations		Active Hit-Call Associations	
	Known MOA	Possible eCBS	Known MOA	Possible eCBS	Endocrine Pathway?	eCBS
	Yes	GABAR, Mito	Yes	DR1, Opioid, Mito	Aromatase Inhibition, AR, ER, TR, GR	Unknown
3COMP EAD_{Human} Predictions[c]	Range: 0.03 to 7.02 mg/kg/day		Range: 0.12 to 16 mg/kg/day		Range: 1.45 to 11 mg/kg/day	
HTTK-Pop AS-EAD_{Human} Predicted vs. AS-ELOEL/LOEL *In Vivo* Measured[d]	Concordant for Selected Assays		± Concordant for Selected Assays		Not Concordant	
HTTK-Pop Fold Difference[d]	Range: 1–5		Range: 12–41		Range: 166–1221 (Supplemental Table 7)	

Abbreviations: AS-LOEL/ELOEL: Allometrically Scaled LOEL/ELOEL: AR: Androgen receptor; DR1: Dopamine receptor; EAD_{Human}: Estimated Administered Dose in humans; eCBS: Endocannabinoid System; ER: Estrogen receptor; GABAR: GABA receptor; GR: Glucocorticoid receptor; Mito: Mitochondrial activity; MOA: Mode of Action.
a- Data in Table 1.
b- Data in Table 3.
c- Data in Table 3; Figs. 1 and 2.
d- Data in Table 4.

HTTK-Pop modeled refinements resulted in higher fold differences for many assays but the results identified relevant targets associated with CPF and CPFO for ages 0–4 (Testai et al., 2010).

5. Discussion

This case study provided an example of how open access CompTox tools might be used to examine *in vitro* targets to characterize metabolic pathways and to determine their EAD in humans for comparison with *in vivo* measured values. Predictions in previous studies, designed to make such comparisons for use in risk assessment, produced a CPF $POD_{50th\ percentile}$ (~LOEL) of 3.55 mg/kg/day and a $POD_{95th\ percentile}$ (~NOEL) of 1.26 mg/kg/day (Friedman et al., 2019). The LOEL predictions were 44-fold greater than the allometrically scaled LOEL for eCBS-related effects in preweaning rats (Carr et al., 2020, Carr et al., 2017, Carr et al., 2014). Hence, we sought to refine the methods with a focus on individual chemical MOAs, and elements withing these pathways that could indicate a tipping point for adverse effects downstream (Saili et al., 2020).

Traditional *in vivo* Health Effects Test Guideline studies used for pesticide registration were designed to reach a low or no effect dose level and, if possible, identify a targeted system (US EPA, 1998). CPF and CPFO were tested in traditional bioassays for risk assessment purposes, hence these data-rich xenobiotics are well-characterized (US EPA, 2020a, US EPA, 2011). Nevertheless, *in vivo* studies, because of the many pathways of toxicity and difficulty in selecting optimal doses to discover the most sensitive POD, are sometimes unreliable and/or hard to interpret. Variability in the selected *in vivo* PODs is dependent on the individual study protocols (e.g., treatment levels, dose spacing, duration, animal strain, chemical route of administration and other factors) determined by study authors. CPF/CPFO are well-characterized toxicologically as AChE inhibitors, however, a combination of their residues on cannabis crops, each affecting the dopaminergic, glutamatergic, and GABAergic neurons, opioid receptors and CB1/mtCB1 receptors, could pose significant neurodevelopmental health risks (Djeungoue-Petga and Hebert-Chatelain, 2017, Fride, 2008, Middlemore-Risher et al., 2011, Wang et al., 2006, Berghuis, 2005, Berghuis et al., 2007). Further research is needed in this area, especially since the eCBS is essential to development from conception to adulthood (Fride, 2008, Mato et al., 2003).

ToxCast/Tox21 results for CPF supported the need for metabolic activation of CPF to the toxic metabolite CPFO for an increase in assay target activation to occur (Testai et al., 2010, Casida et al., 2008). This was evident in that CPFO had many more active hit-calls than CPF with endpoints relevant to the known metabolic pathway. Since CPF/CPFO and $^{\Delta 9}$THC overlap in their metabolic pathways, targets with CPF/CPFO active hit-calls, could also affect $^{\Delta 9}$THC metabolism. The balance between CPF/CPFO and $^{\Delta 9}$THC availability in the brain after activation/detoxification, along with their exposure levels could determine their levels of agonistic behavior at the CB1 receptor. In addition, the main $^{\Delta 9}$THC metabolic pathway involves CYP2C9 and CYP3A in Phase I metabolism and glucuronidation (UGT1A1) via oxidation to THC-COOH-glucuronide (Huestis, 2005, Mazur et al., 2009, Dinis-Oliveira, 2016). Where CPFO is metabolically activated by these CYPS, $^{\Delta 9}$THC is detoxified (Huestis, 2005, Dinis-Oliveira, 2016). CPFO is detoxified by PON-1 which is not involved with the $^{\Delta 9}$THC pathway. The degree to which each CYP is induced is dependent on the exposure (dose) of both chemicals. Induction of the same P450s by both chemicals could potentially reach a tipping point at lower doses compared with exposure to a single compound (Saili et al., 2020). Other variables include frequency and duration of exposure because chronic intake may lead to higher hepatic or systemic levels of the CYPs and the sensitivity, age, genetic makeup, health status, diet and other factors relating to exposed individuals (Hewitt et al., 2007, Bernasconi et al., 2019). These factors are often difficult to characterize in humans since hepatic metabolism studies are, by necessity, generally performed *in vitro* (Bernasconi et al., 2019).

CPF had an active hit call in a GABA receptor assay, CPFO had active hit-calls for a dopamine receptor and two opiate receptor assays and both compounds had active hit-calls with mitochondrial assays. CPF and CPFO have known *in vivo* associations with effects on these targets in the brain and in the eCBS during development (Aldridge et al., 2005, Slotkin and Seidler, 2007, Alugubelly et al., 2021, Carr et al., 2020, Carr et al., 2014, Middlemore-Risher et al., 2011). While *in vivo* links have been shown, the data from ToxCast/Tox21 were weak and did not directly support an association of either chemical with these pathways. There were also no active hit-calls for $^{\Delta 9}$THC for GABA, dopamine, opioid receptors, or mitochondrial targets, these are among the most vulnerable targets affected by $^{\Delta 9}$THC exposure *in vivo*, especially during development (Berghuis, 2005, Berghuis et al., 2007, Fernández-Ruiz et al., 2019, Navarro et al., 1996, Fernández-Ruiz et al., 2004, Bénard et al., 2012, Djeungoue-Petga and Hebert-Chatelain, 2017).

$^{\Delta 9}$THC had only two active hit-calls in ToxCast/Tox21 below the cytotoxicity limit and these were related to cell stress, associated with cytotoxicity. Most of the $^{\Delta 9}$THC assays tested were for cytotoxicity, cell stress or cell-stress-related assay interference and not specific to $^{\Delta 9}$THC biological activity or to the metabolic pathway. All $^{\Delta 9}$THC assays were performed only with the Tox21 (NCGC) vendor (Supplemental Table 3). The lack of active hit-calls with $^{\Delta 9}$THC was likely due to not having assays specific to the metabolic pathway to characterize $^{\Delta 9}$THC activity (e.g., CB1 receptor). Without such assays, the available ToxCast/Tox21 assays may not provide useful information on key mechanistic steps in the $^{\Delta 9}$THC MOA.

It is well-documented that $^{\Delta 9}$THC affects the CNS in animal models and humans throughout development and in adulthood through several routes of exposure (Di Marzo, 2011, Di Marzo et al., 2008, Berghuis, 2005, Berghuis et al., 2007, Bloomfield et al., 2016, Borowska et al., 2018, Bruijnzeel et al., 2019, Calvigioni et al., 2014, Hložek et al., 2017). However, the data for this study indicated that Toxcast/Tox21 assays do not provide insights on the effect of $^{\Delta 9}$THC on the eCBS or other areas of the CNS. The lack of availability of assays for reactions more specific to eCBS toxicity also limited data interpretation. $^{\Delta 9}$THC may have weak effects on male and female reproduction acting through the eCBS (Lee et al., 2020, Payne et al., 2019) or the effects may be non-specific due to lipophilicity. Additional work is needed to tease out the significance of the endocrine-related active hit-calls. The United States Food and Drug Administration has been studying the science of cannabis for medical uses, and as of 2021, no marketing application for cannabis treatment for medical conditions or diseases has been approved. However, one cannabis-derived and three cannabis-related drugs are available only by prescription from licensed health providers (FDA Regulation of Cannabis and Cannabis-Derived Products, Including Cannabidiol (CBD) | FDA).

The HTTK 3COMP and PBTK models were designed to provide alternatives to animal testing for chemical safety, in support of the US EPA drive to eliminate animal testing by 2035 (US EPA, 2020b). They are also used to validate and support new approach methodologies (NAM) to chemical risk assessment and toxicity characterization (Prior et al., 2019). The NAMs address ethical concerns, involving "…implementation of the 3Rs – replacement, refinement and reduction of the use of animals," as well as scientific, financial and regulatory issues (Prior et al., 2019). HTTK 3COMP and PBTK methods, along with the NAMs provide easy-to-use, open access computational tools to connect *in vitro* bioactivity as seen with ToxCast/Tox21 data to PODs measured *in vivo*. In this study we were able to explore these oral models to see how closely they predicted PODs observed *in vivo*.

Qualitatively and quantitatively the 3COMP model, with AS interspecies extrapolation, provided the more predictive EAD_{Human} values. This result indicated model complexity (e.g., PBTK) did not necessarily provide better predictions. An appropriate model at the level of

ranking or prioritizing toxicity was provided by the simpler 3COMP model. However, interpretation of the predictiveness of modeled EAD_{Human} values must take into consideration several factors, including relevance of an assay to the MOA/eCBS, availability of metabolic activation to generate a representative chemical-target interaction and AC_{50}s value in relation to the cytotoxicity limit. Simply having a predictive fold difference is not enough to ensure the EAD_{Human} is predictive.

HTTK-Pop model estimations resulted from Monte Carlo sampling of NHANES physiological, body weight and age-related parameters (Wambaugh et al., 2018, Wambaugh et al., 2019). The output of HTTK-Pop for a given population subgroup is the median (i.e., 50th quantile), hence, the age specific HTTK-Pop EAD_{Human} has its own distribution. HTTK-Pop EAD_{Human} calculations were adjusted for ages 0–80, but the subpopulation under consideration for this study was 0–4 years based on the animal to human age adjustments (Sengupta (2011), Sengupta (2013); Supplemental Table 7 HTTK-Pop data for all ages). HTTK-Pop incorporated PK values and can only address the PK differences among various population subgroups based on their variations in metabolic capabilities. Pharmacodynamic (PD) parameters (i.e., effects of a chemical on the body) measure what the body does to a chemical that will ultimately translate into a toxicological response (Meibohm and Derendorf, 1997). However, PD modeling requires the toxicity mechanism to be definitively identified (e.g., cholinesterase inhibition), and such a model has not been developed for endocannabinoid effects for CPF/CPFO or $^{\Delta 9}$THC.

The HTTK-Pop model for ages 0–4 have the same issues with data interpretation as already described. Fewer assays had predictive PODs with adjustments for age for CPF and CPFO and there were no predictive HTTK-Pop EAD_{Human} for $^{\Delta 9}$THC. This is likely due, in part to the fact that the EAD_{Human} in young children are predicted to be higher than adults as was seen in this study (Supplemental Table 7) (Ginsberg et al., 2002, Ginsberg et al., 2004). Older ages have lower EAD_{Human} predictions that are closer to the AS-ELOEL/LOELs (Data shown in Supplemental Table 7).

While the modeled EAD_{Humans} values in this study may not, in some cases be highly predictive, it is evident that metabolic activation in ToxCast/Tox21 assays remains an issue for some chemicals to produce an active hit-call below the cytotoxicity limit. It also calls attention to the need for an increased variety of assays to assess biological activities that are not currently available on the CompTox Dashboard, as was shown with $^{\Delta 9}$THC. Assays for CB1 and CB2 receptors, FAAH and MAGL, are not only important for characterizing $^{\Delta 9}$THC but also for assessing other cannabinoid pathways (e.g., cannabidiol: CBD) and eCBS-affected CPF toxicity during development (Araujo et al., 2019, Di Marzo and Silvestri, 2019, Carr et al., 2020, Carr et al., 2017, Carr et al., 2014). Endocannabinoids are involved in neural development from embryogenesis through adolescence in the developing human brain (Berghuis et al., 2007, de Salas-Quiroga et al., 2015, de Salas-Quiroga et al., 2020). CPF/CPFO and $^{\Delta 9}$THC disrupt the eCBS throughout development with neurotoxic consequences, including decreased cognition, working memory and locomotor activity (de Salas-Quiroga et al., 2015, de Salas-Quiroga et al., 2020, Grant et al., 2018, Rauh et al., 2011, Silva, 2020). CPF exposure is also associated with ASD in animals (De Felice et al., 2015, De Felice et al., 2014) and in children exposed prenatally (Shelton et al., 2014). While $^{\Delta 9}$THC is not directly associated with ASD, when co-exposure with CPF/CPFO residues on cannabis occurs during development, there could be combined neurotoxicity leading to ASD.

On the other hand, cannabidiol (CBD: 2nd highest concentration in cannabis) (Atakan, 2012) has been used to treat symptoms of neurotoxic diseases like ASD and epilepsy (Fleury-Teixeira et al., 2019, Poleg et al., 2019, Pretzsch et al., 2019). CBD potentially acts through microglia in the brain (Poleg et al., 2019, Pretzsch et al., 2019). Microglia are CNS immune cells associated with mediation of neuroinflammation and are instrumental in shaping and regulating neuronal synapses during development (Butovsky and Weiner, 2018). Disruptions during development have been linked to inflammation linked to ASD (Araujo et al., 2019). Microglia have an abundance of immune-response-associated CB2 receptors that, when stimulated, inhibit microglial activation, and promote an anti-inflammatory, neuroprotective response (Stella, 2009). While there is no direct link between eCBS and ASD, CBD has been shown to block activation of microglia and inhibit neuroinflammation linked to seizures and ASD (Elliott et al., 2018, Maroon and Bost, 2018, Martín-Moreno et al., 2011, Poleg et al., 2019, Pretzsch et al., 2019). These findings stress the importance of developing *in vitro* high throughput assays to identify upstream initiating events or adverse outcome pathways to explore disease-related molecular events for drug development (e.g., CBD) or for use in chemical risk assessment. Modeled predicted PODs associated with common targets within metabolic pathways (e.g., AhR shared between CPF and $^{\Delta 9}$THC) could provide insights into the effects of combined exposures to pesticides and cannabis.

6. Conclusions

The CompTox tools used in this case study are versatile and allow for a great deal of refinements for determination of EAD_{Human} PODs that could be used for risk assessment. It is critical however, that each step in the evaluation be carefully reviewed for biological relevance. As with $^{\Delta 9}$THC, the 3COMP EAD_{Human} PODs appeared predictive, but were not biologically meaningful based on the ToxCast/Tox21 active hit-call targets that were primarily unrelated to the MOA or eCBS and their AC_{50} values that exceeded the cytotoxicity limit. Nevertheless, it is the goal the US EPA and international regulatory bodies to use new approach methodologies (NAM) and CompTox tools to eventually replace *in vivo* toxicity tests (US EPA, 2020b; OECD adopts new Guideline on Defined Approaches on Skin Sensitisation | ALTEX - Alternatives to animal experimentation; accessed 8/2021). A variety of NAMs performed in cells or zebrafish, for example, skin sensitization, and endocrine active substance tests are currently being employed for this purpose (OECD, 2021a, OECD, 2021b). ToxCast/Tox21 data have been used to build a vascular developmental Adverse Outcome Pathway to predict embryonic vascular disruption (Saili et al., 2019). Further, an interagency/international initiative was organized to use new approach methodologies such as ToxCast/Tox21, HTTK 3COMP, PBTK and HTTK-Pop models to predict EAD_{Human} for the purpose of risk assessment (Friedman, 2019, Friedman et al., 2019). These models are presently used in combination with open access traditional *in vivo* studies from sources such as the Toxicity Reference Database (ToxRefDB) and the Toxicity Value Database (ToxValDB with >40 sources, including ToxRefDB) (Martin et al., 2011, Williams et al., 2017). With the development of new assays related to the eCBS, it could be possible to investigate common biological components between cannabis/$^{\Delta 9}$THC and pesticide contaminants. With the development of new CompTox tools some of the roadblocks to data interpretation can be resolved.

Funding

This research did not receive any specific grant from funding agencies in the public, commercial, or not-for-profit sectors.

CRediT authorship contribution statement

Marilyn Silva: Supervision, Conceptualization, Investigation, Resources, Visualization, Methodology, Writing – original draft, Writing – review & editing, Data curation. **Ryan Kin-Hin Kwok:** Conceptualization, Investigation, Resources, Visualization, Methodology, Writing – original draft, Writing – review & editing, Software, Formal analysis.

Declaration of Competing Interest

The authors declare that they have no known competing financial interests or personal relationships that could have appeared to influence the work reported in this paper.

Acknowledgements

I would like to thank Dr. John Wambaugh, PhD, from the US EPA for his continued help and support with the HTTK and HTTK-Pop models. I thank Dr. Eric S.C. Kwok, PhD, DABT, CalEPA for his helpful reviews and comments of this manuscript. I would also like to thank Dr. Richard Judson, PhD, US EPA, for feedback on ToxCast data analysis.

Appendix A. Supplementary data

Supplementary data to this article can be found online at https://doi.org/10.1016/j.crtox.2022.100064.

References

Ahn, K., McKinney, M.K., Cravatt, B.F., 2008. Enzymatic pathways that regulate endocannabinoid signaling in the nervous system. Chem. Rev. 108 (5), 1687–1707.
Aldridge, J.E., Meyer, A., Seidler, F.J., Slotkin, T.A., 2005. Alterations in central nervous system serotonergic and dopaminergic synaptic activity in adulthood after prenatal or neonatal chlorpyrifos exposure. Environ. Health Perspect. 113, 1027–1031.
Allegaert, K., van den Anker, J., 2019. Ontogeny of phase I metabolism of drugs. J. Clin. Pharmacol. 59, S33–S41.
Alugubelly, N., Mohammed, A.N., Carr, R.L., 2021. Persistent proteomic changes in glutamatergic and GABAergic signaling in the amygdala of adolescent rats exposed to chlorpyrifos as juveniles. NeuroToxicology 85, 234–244.
Araujo, D.J., Tjoa, K., Saijo, K., 2019. The endocannabinoid system as a window into microglial biology and its relationship to autism. Front. Cell. Neurosci. 13.
Atakan, Z., 2012. Cannabis, a complex plant: different compounds and different effects on individuals. Therap. Adv. Psychopharmacol. 2, 241–254.
Badée, J., Fowler, S., de Wildt, S.N., Collier, A.C., Schmidt, S., Parrott, N., 2019. The ontogeny of UDP-glucuronosyltransferase enzymes, recommendations for future profiling studies and application through physiologically based pharmacokinetic modelling. Clin. Pharmacokinet. 58, 189–211.
Baker, T., Datta, P., Rewers-Felkins, K., Thompson, H., Kallem, R.R., Hale, T.W., 2018. Transfer of inhaled cannabis into human breast milk. Obstet. Gynecol. 131, 783–788.
Bell, S.M., Abedini, J., Ceger, P., Chang, X., Cook, B., Karmaus, A.L., et al, 2020. An integrated chemical environment with tools for chemical safety testing. Toxicol. In Vitro 67, 104916.
Bell, S.M., Chang, X., Wambaugh, J.F., Allen, D.G., Bartels, M., Brouwer, K.L.R., et al, 2018. In vitro to in vivo extrapolation for high throughput prioritization and decision making. Toxicol. In Vitro 47, 213–227.
Bénard, G., Massa, F., Puente, N., Lourenço, J., Bellocchio, L., Soria-Gómez, E., et al, 2012. Mitochondrial CB 1 receptors regulate neuronal energy metabolism. Nat. Neurosci. 15, 558–564.
Benard, G., Massa, F., Puente, N., Lourenco, J., Bellocchio, L., Soria-Gomez, E., et al, 2012. Mitochondrial CB 1 receptors regulate neuronal energy metabolism. Nat. Neurosci. 15, 558.
Berghuis, P., 2005. Brain-derived Neurotrophic Factor and Endocannabinoid Functions in GABAergic Interneuron Development. Karolinska Instituet, Stockholm, p. 2007.
Berghuis, P., Rajnicek, A.M., Morozov, Y.M., Ross, R.A., Mulder, J., Urbán, G.M., et al, 2007. Hardwiring the brain: endocannabinoids shape neuronal connectivity. Science 316, 1212–1216.
Bernasconi, C., Pelkonen, O., Andersson, T.B., Strickland, J., Wilk-Zasadna, I., Asturiol, D., et al, 2019. Validation of in vitro methods for human cytochrome P450 enzyme induction: Outcome of a multi-laboratory study. Toxicol. In Vitro 60, 212–228.
Berridge, K.C., Ho, C.-Y., Richard, J.M., Difeliceantonio, A.G., 2010. The tempted brain eats: Pleasure and desire circuits in obesity and eating disorders. Brain Res. 1350, 43–64.
Bessems, J.G., Loizou, G., Krishnan, K., Clewell, H.J., Bernasconi, C., Bois, F., et al, 2014. PBTK modelling platforms and parameter estimation tools to enable animal-free risk assessment: Recommendations from a joint EPAA – EURL ECVAM ADME workshop. Regul. Toxicol. Pharm. 68, 119–139.
Bloomfield, M.A.P., Ashok, A.H., Volkow, N.D., Howes, O.D., 2016. The effects of Δ9-tetrahydrocannabinol on the dopamine system. Nature 539, 369–377.
Borowska, M.A.C., Sawicka-Gutaj, N., Woliński, K., Płazińska, M.-T., Mikołajczak, P., Ruchała, M., 2018. The effects of cannabinoids on the endocrine system. Endokrynologia Polska 69, 705–719.
Breen, M., Ring, C.L., Kreutz, A., Goldsmith, M.-R., Wambaugh, J.F., 2021. High-throughput PBTK models for in vitro to in vivo extrapolation. Expert Opin. Drug Metab. Toxicol. 17 (8), 903–921.
Bruijnzeel, A.W., Knight, P., Panunzio, S., Xue, S., Bruner, M.M., Wall, S.C., et al, 2019. Effects in rats of adolescent exposure to cannabis smoke or THC on emotional behavior and cognitive function in adulthood. Psychopharmacology 236, 2773–2784.
Butovsky, O., Weiner, H.L., 2018. Microglial signatures and their role in health and disease. Nat. Rev. Neurosci. 19, 622–635.
Calvigioni, D., Hurd, Y.L., Harkany, T., Keimpema, E., 2014. Neuronal substrates and functional consequences of prenatal cannabis exposure. Eur. Child Adolesc. Psychiatry 23, 931–941.
Carr, R.L., Alugubelly, N., de Leon, K., Loyant, L., Mohammed, A.N., Patterson, M.E., et al, 2020. Inhibition of fatty acid amide hydrolase by chlorpyrifos in juvenile rats results in altered exploratory and social behavior as adolescents. NeuroToxicology 77, 127–136.
Carr, R.L., Armstrong, N.H., Buchanan, A.T., Eells, J.B., Mohammed, A.N., Ross, M.K., et al, 2017. Decreased anxiety in juvenile rats following exposure to low levels of chlorpyrifos during development. NeuroTox 59, 183–190.
Carr, R.L., Graves, C.A., Mangum, L.C., Nail, C.A., Ross, M.K., 2014. Low level chlorpyrifos exposure increases anandamide accumulation in juvenile rat brain in the absence of brain cholinesterase inhibition. Neurotoxicology 43, 82–89.
Casida, J.E., 2017. Organophosphorus xenobiotic toxicology. Annu. Rev. Pharmacol. Toxicol. 57, 309–327.
Casida, J.E., Nomura, D.K., Vose, S.C., Fujioka, K., 2008. Organophosphate-sensitive lipases modulate brain lysophospholipids, ether lipids and endocannabinoids. Chem. Biol. Interact. 175, 355–364.
CDPR, 2018. Evaluation of Chlorpyrifos as a Toxic Air Contaminant: Addendum to the Risk Characterization of Spray Drift, Dietary, and Aggregate Exposures to Residential Bystanders Human. Human Health Assessment Branch, Department of Pesticide Regulation, California Environmental Protection Agency, Sacramento, CA. http://www.cdpr.ca.gov/docs/whs/active_ingredient/chlorpyrifos.htm.
Cha, Y.M., White, A.M., Kuhn, C.M., Wilson, W.A., Swartzwelder, H.S., 2006. Differential effects of delta9-THC on learning in adolescent and adult rats. Pharmacol. Biochem. Behav. 83, 448–455.
Chang, T.K.H., Bandiera, S.M., Chen, J., 2003. Constitutive androstane receptor and pregnane X receptor gene expression in human liver: interindividual variability and correlation with CYP2B6 mRNA levels. Drug Metab. Dispos. 31, 7.
Chiu, K.-C., Sisca, F., Ying, J.-H., Tsai, W.-J., Hsieh, W.-S., Chen, P.-C., et al, 2021. Prenatal chlorpyrifos exposure in association with PPARγ H3K4me3 and DNA methylation levels and child development. Environ. Pollut. 274, 116511.
Choi, S., Yoo, S., Lee, B., 2004. Toxicological characteristics of endocrine-disrupting chemicals: developmental toxicity, carcinogenicity, and mutagenicity. J. Toxicol. Environ. Health Part B, Crit. Rev. 7, 1–24.
DBH, 2022. Marijuana Use Statistics Around the World 2019. Delphi Behavioral Health Group Weekly Newsletter. 1/2022 esd. Fort Lauderdale, Florida: Delphi Behavioral Health Group.
de Felice, A., Scattoni, M.L., Ricceri, L., Calamandrei, G., 2015. Prenatal exposure to a common organophosphate insecticide delays motor development in a mouse model of idiopathic autism. PLoS ONE 10, e0121663.
de Felice, A., Venerosi, A., Ricceri, L., Sabbioni, M., Scattoni, M.L., Chiarotti, F., et al, 2014. Sex-dimorphic effects of gestational exposure to the organophosphate insecticide chlorpyrifos on social investigation in mice. Neurotoxicol. Teratol. 46, 32–39.
De Salas-Quiroga, A., Díaz-Alonso, J., García-Rincón, D., Remmers, F., Vega, D., Gómez-Cañas, M., et al, 2015. Prenatal exposure to cannabinoids evokes long-lasting functional alterations by targeting CB1 receptors on developing cortical neurons. PNAS 112, 13693–13698.
De Salas-Quiroga, A., García-Rincón, D., Gómez-Domínguez, D., Valero, M., Simón-Sánchez, S., Paraíso-Luna, J., et al, 2020. Long-term hippocampal interneuronopathy drives sex-dimorphic spatial memory impairment induced by prenatal THC exposure. Neuropsychopharmacology 45, 877–886.
Di Marzo, V., 2011. Endocannabinoid System. Wiley Online Library.
Di Marzo, V., Côté, M., Matias, I., Lemieux, I., Arsenault, B.J., Cartier, A., et al, 2008. Changes in plasma endocannabinoid levels in viscerally obese men following a 1 year lifestyle modification programme and waist circumference reduction: associations with changes in metabolic risk factors. Diabetologia 52, 213.
Di Marzo, V., Piscitelli, F. & Mechoulam, R. 2011. Cannabinoids and Endocannabinoids in Metabolic Disorders with Focus on Diabetes. In: Schwanstecher, M. (esd.) Diabetes – Perspectives in Drug Therapy. Berlin, Heidelberg: Springer Berlin Heidelberg.
Di Marzo, V., Silvestri, C., 2019. Lifestyle and metabolic syndrome: contribution of the endocannabinoidome. Nutrients 11, 1956–1970.
Dinis-Oliveira, R.J., 2016. Metabolomics of Δ9-tetrahydrocannabinol: implications in toxicity. Drug Metab. Rev. 48, 80–87.
Djeungoue-Petga, M.-A., Hebert-Chatelain, E., 2017. Linking mitochondria and synaptic transmission: the CB1 receptor. BioEssays 39, 1700126.
Dow-Edwards, D., Zhao, N., 2008. Oral THC produces minimal behavioral alterations in preadolescent rats. Neurotoxicol. Teratol. 30, 385–389.
Dryburgh, L.M., Bolan, N.S., Grof, C.P.L., Galettis, P., Schneider, J., Lucas, C.J., et al, 2018. Cannabis contaminants: sources, distribution, human toxicity and pharmacologic effects. Br. J. Clin. Pharmacol. 84, 2468–2476.
Eaton, D.L., Daroff, R.B., Autrup, H., Bridges, J., Buffler, P., Costa, L.G., et al, 2008. Review of the toxicology of chlorpyrifos with an emphasis on human exposure and neurodevelopment. Crit. Rev. Toxicol. 38 (Suppl 2), 1–125.
EFSA, 2014. Conclusion on the peer review of the pesticide human health risk assessment of the active substance chlorpyrifos. Eur. Food Safety Authority J. 12, 3640–3674.

EFSA, 2015. EFSA panel on contaminants in the food chain: scientific opinion on the risks for human health related to the presence of tetrahydrocannabinol (THC) in milk and other food of animal origin. EFSA J. 13, 4141.
El-Masri, H., Kleinstreuer, N., Hines, R.N., Adams, L., Tal, T., Isaacs, K., et al, 2016. Integration of life-stage physiologically based pharmacokinetic models with adverse outcome pathways and environmental exposure models to screen for environmental hazards. Toxicol. Sci. 152 (1), 230–243.
Elliott, D.M., Singh, N., Nagarkatti, M., Nagarkatti, P.S., 2018. Cannabidiol attenuates experimental autoimmune encephalomyelitis model of multiple sclerosis through induction of myeloid-derived suppressor cells. Front. Immunol. 9.
Elsohly, M.A., 2002. Chemical Constituents of Cannabis. Haworth Press, New York.
Fergusson, D.M., Horwood, L.J., Northstone, K., Team, A.S., 2002. Maternal use of cannabis and pregnancy outcome. BJOG: Int. J. Obstetrics Gynaecol. 109, 21–27.
Fernández-Ruiz, J.J., Gómez, M., Hernández, M., de Miguel, R., Ramos, J.A., 2004. Cannabinoids and gene expression during brain development. Neurotox. Res. 6, 389–401.
Fernández-ruiz, J.J., Rodriguez de Fonseca, F., Navarro, M., Ramos, J.A., 2019. Maternal Cannabinoid Exposure and Brain Development: Changes in the Ontogeny of Dopaminergic Neurons. CRC Press, Marijuana/cannabinoids.
Fernandez, E., Perez, R., Hernandez, A., Tejada, P., Arteta, M., Ramos, J.T., 2011. Factors and mechanisms for pharmacokinetic differences between pediatric population and adults. Pharmaceutics 3, 53–72.
Filer, D.L., Kothiya, P., Setzer, R.W., Judson, R., Martin, M.T., 2017. tcpl: the ToxCast pipeline for high-throughput screening data. Bioinformatics 33, 618–620.
Fleury-Teixeira, P., Caixeta, F.V., Ramires da Silva, L.C., Brasil-Neto, J.P., Malcher-Lopes, R., 2019. Effects of CBD-enriched cannabis sativa extract on autism spectrum disorder symptoms: an observational study of 18 participants undergoing compassionate use. Front. Neurol. 10.
Fortin, D.A., Levine, E.S., 2007. Differential effects of endocannabinoids on glutamatergic and GABAergic inputs to layer 5 pyramidal neurons. Cereb. Cortex 17, 163–174.
Foxenberg, R.J., Ellison, C.A., Knaak, J.B., Ma, C., Olson, J.R., 2011. Cytochrome P450-specific human PBPK/PD models for the organophosphorus pesticides: chlorpyrifos and parathion. Toxicology 285 (1-2), 57–66.
Foxenberg, R.J., McGarrigle, B.P., Knaak, J.B., Kostyniak, P.J., Olson, J.R., 2007. Human hepatic cytochrome P450-specific metabolism of parathion and chlorpyrifos. Drug Metab. Dispos. 35, 189.
Frank, C.L., Brown, J.P., Wallace, K.B., Wambaugh, J.F., Shah, I., Shafer, T.J., 2018. Defining toxicological tipping points in neuronal network development. Toxicol. Appl. Pharmacol. 354, 81–93.
Fride, E., 2004. The endocannabinoid-CB1 receptor system in pre- and postnatal life. Eur. J. Pharmacol. 500, 289–297.
Fride, E., 2008. Multiple roles for the endocannabinoid system during the earliest stages of life: pre- and postnatal development. J. Neuroendocrinol. 20, 75–81.
Fried, P.A., Smith, A.M., 2001. A literature review of the consequences of prenatal marihuana exposure. An emerging theme of a deficiency in aspects of executive function. Neurotoxicol. Teratol. 23, 1–11.
Friedman, K.P. 2019. Quantitative variability in repeat dose toxicity studies: Implications for scientific confidence in NAMs Office of Research and Development, Center for Computational Toxicology & Exposure (CCTE; Bioinformatic and Computational Toxicology Division (BCTD) and Computational Toxicology and Bioinformatics Branch (CTBB) State of the Science on Development and Use of New Approach Methods (NAMs) for Chemical Safety Testing: December 17, 2019.
Friedman, K.P., Gagne, M., Loo, L.H., Karamertzanis, P., Netzeva, T., Sobanski, T., et al, 2019. Utility of in vitro bioactivity as a lower bound estimate of in vivo adverse effect levels and in risk-based prioritization. Toxicol. Sci. https://doi.org/10.1093/toxsci/kfz201/5571376.
Ginsberg, G., Hattis, D., Sonawane, B., Russ, A., Banati, P., Kozlak, M., et al, 2002. Evaluation of child/adult pharmacokinetic differences from a database derived from the therapeutic drug literature. Toxicol. Sci. 66, 185–200.
Gómez-Giménez, B., Felipo, V., Cabrera-Pastor, A., Agustí, A., Hernández-Rabaza, V., Llansola, M., 2018. Developmental exposure to pesticides alters motor activity and coordination in rats: sex differences and underlying mechanisms. Neurotox. Res. 33 (2), 247–258.
Ginsberg, G., Slikker Jr., W., Bruckner, J., Sonawane, B., 2004. Incorporating children's toxicokinetics into a risk framework. Environ. Health Perspect. 112, 272–283.
Grant, K.S., Petroff, R., Isoherranen, N., Stella, N., Burbacher, T.M., 2018. Cannabis use during pregnancy: pharmacokinetics and effects on child development. Pharmacol. Ther. 182, 133–151.
Haj-Dahmane, S., Shen, R.-Y., 2010. Regulation of plasticity of glutamate synapses by endocannabinoids and the cyclic-AMP/protein kinase A pathway in midbrain dopamine neurons. J. Physiol. 588 (14), 2589–2604.
Herriage, S., Chen, G.G., Pope, C., 2022. Concentration-dependent effects of chlorpyrifos oxon on peroxisome proliferator-activated receptor signaling in MCF-7 cells. Toxicol. In Vitro 78, 105268.
Hewitt, N.J., Lecluyse, E.L., Ferguson, S.S., 2007. Induction of hepatic cytochrome P450 enzymes: methods, mechanisms, recommendations, and in vitro–in vivo correlations. Xenobiotica 37, 1196–1224.
Hines, R.N., 2008. The ontogeny of drug metabolism enzymes and implications for adverse drug events. Pharmacol. Ther. 118, 250–267.
Hložek, T., Uttl, L., Kaderõábek, L., Balíková, M., Lhotková, E., Horsley, R.R., et al, 2017. Pharmacokinetic and behavioural profile of THC, CBD, and THC + CBD combination after pulmonary, oral, and subcutaneous administration in rats and confirmation of conversion in vivo of CBD to THC. Eur. Neuropsychopharmacol. 27 (12), 1223–1237.
Holick, M.F., 2005. Stay tuned to PXR: an orphan actor that may not be D-structive only to bone. J. Clin. Investig. 115, 32–34.
Howlett, A.C., Barth, F., Bonner, T.I., Cabral, G., Casellas, P., Devane, W.A., et al, 2002. International Union of Pharmacology. XXVII. Classification of cannabinoid receptors. Pharmacol. Rev. 54, 161–202.
Huestis, M.A., 2005. Pharmacokinetics and metabolism of the plant cannabinoids, delta9-tetrahydrocannabinol, cannabidiol and cannabinol. Handb. Exp. Pharmacol., 657–690.
Iannotti, F.A., Vitale, R.M., 2021. The endocannabinoid system and PPARs: focus on their signalling crosstalk, action and transcriptional regulation. Cells 10 (3), 586. https://doi.org/10.3390/cells10030586.
ICE 2021. ICE IVIVE Tool. https://ntp.niehs.nih.gov/whatwestudy/niceatm/comptox/ct-ice/ice.html, Accessed 9-2020.
Judge, S.J., Savy, C.Y., Campbell, M., Dodds, R., Gomes, L.K., Laws, G., et al, 2016. Mechanism for the acute effects of organophosphate pesticides on the adult 5-HT system. Chem. Biol. Interact. 245, 82–89.
Judson, R., Houck, K., Martin, M., Richard, A.M., Knudsen, T.B., Shah, I., et al, 2016. Analysis of the effects of cell stress and cytotoxicity on in vitro assay activity across a diverse chemical and assay space. Toxicol. Sci. 152, 323–339.
Judson, R.S., Houck, K.A., Kavlock, R.J., Knudsen, T.B., Martin, M.T., Mortensen, H. M., et al, 2010. In vitro screening of environmental chemicals for targeted testing prioritization: the ToxCast project. Environ. Health Persp. 118 (4), 485–492.
Judson, R., Kavlock, R.J., Setzer, R.W., Hubal, E.A.C., Martin, M.T., Knudsen, T.B., et al, 2011. Estimating toxicity-related biological pathway altering doses for high-throughput chemical risk assessment. Chem. Res. Toxicol. 24, 451–462.
Katona, I., Freund, T.F., 2012. Multiple functions of endocannabinoid signaling in the brain. Annu. Rev. Neurosci. 35, 529–558.
Kirilly, E., Hunyady, L., Bagdy, G., 2013. Opposing local effects of endocannabinoids on the activity of noradrenergic neurons and release of noradrenaline: relevance for their role in depression and in the actions of CB 1 receptor antagonists. J. Neural Transm. 120, 177–186.
Korpi, E.R., den Hollander, B., Farooq, U., Vashchinkina, E., Rajkumar, R., Nutt, D.J., et al, 2015. Mechanisms of action and persistent neuroplasticity by drugs of abuse. Pharmacol. Rev. 67, 872–1004.
Lee, M.S., Lanes, A., Ginsburg, E.S., Fox, J.H., 2020. Delta-9 THC can be detected and quantified in the semen of men who are chronic users of inhaled cannabis. J. Assist. Reprod. Genet. 37 (6), 1497–1504.
Leung, M.C.K., Silva, M.H., Palumbo, A.J., Lohstroh, P.N., Koshlukova, S.E., Duteaux, S. B., 2019. Adverse outcome pathway of developmental neurotoxicity resulting from prenatal exposures to cannabis contaminated with organophosphate pesticide residues. Reprod. Toxicol. 85, 12–18.
Li, J., Wang, L., Guo, H., Shi, L., Zhang, K., Tang, M., et al, 2017. Targeted sequencing and functional analysis reveal brain-size-related genes and their networks in autism spectrum disorders. Mol. Psychiatry 22, 1282–1290.
Liu, L., Xu, Y., Xu, L., Wang, J., Wu, W., Xu, L., et al, 2015. Analysis of differentially expressed proteins in zebrafish (Danio rerio) embryos exposed to chlorpyrifos. Comp. Biochem. Physiol. C: Toxicol. Pharmacol. 167, 183–189.
Lüscher, C., Ungless, M.A., 2006. The mechanistic classification of addictive drugs. PLoS Med. 3, e437.
Maroon, J., Bost, J. 2018. Review of the neurological benefits of phytocannabinoids. Surgical Neurol. Int., 9, 91–91.
Martín-Moreno, A.M., Reigada, D., Ramírez, B.G., Mechoulam, R., Innamorato, N., Cuadrado, A., et al, 2011. Cannabidiol and other cannabinoids reduce microglial activation in vitro and in vivo: relevance to Alzheimer's disease. Mol. Pharmacol. 79, 964–973.
Martin, M.T., Judson, R.J., Reif, D.M., Kavlock, R.J., Dix, D.J., 2009. Profiling chemicals based on chronic toxicity results from the U.S. EPA ToxRef Database. Environ. Health Perspectives 117, 392–399.
Martin, M.T., Knudsen, T.B., Reif, D.M., Houck, K.A., Judson, R.S., Kavlock, R.J., et al, 2011. Predictive model of rat reproductive toxicity from toxcast high throughput screening1. Biol. Reprod. 85, 327–339.
Mato, S., del Olmo, E., Pazos, A., 2003. Ontogenetic development of cannabinoid receptor expression and signal transduction functionality in the human brain. Eur. J. Neurosci. 17, 1747–1754.
Mazur, A., Lichti, C.F., Prather, P.L., Zielinska, A.K., Bratton, S.M., Gallus-Zawada, A., et al, 2009. Characterization of human hepatic and extrahepatic UDP-glucuronosyltransferase enzymes involved in the metabolism of classic cannabinoids. Drug Metab. Dispos 37, 1496–1504.
McNally, K., Cotton, R., Hogg, A., Loizou, G., 2014. PopGen: A virtual human population generator. Toxicology 315, 70–85.
Medina-Cleghorn, D., Heslin, A., Morris, P.J., Mulvihill, M.M., Nomura, D.K., 2014. Multidimensional profiling platforms reveal metabolic dysregulation caused by organophosphorus pesticides. ACS Chem. Biol. 9, 423–432.
Medina-Díaz, I.M., Rubio-Ortíz, M., Martínez-Guzmán, M.C., Dávalos-Ibarra, R.L., Rojas-García, A.E., Robledo-Marenco, M.L., et al, 2011. Organophosphate pesticides increase the expression of alpha glutathione S-transferase in HepG2 cells. Toxicol. In Vitro 25, 2074–2079.
Meibohm, B., Derendorf, H., 1997. Basic concepts of pharmacokinetic/pharmacodynamic (PK/PD) modelling. Int. J. Clin. Pharmacol. Ther. 35, 401–413.
Michalik, L., Auwerx, J., Berger, J.P., Chatterjee, V.K., Glass, C.K., Gonzalez, F.J., et al, 2006. International Union of Pharmacology. LXI. Peroxisome proliferator-activated receptors. Pharmacol. Rev. 58, 726–741.
Middlemore-Risher, M.-L., Adam, B.-L., Lambert, N.A., Terry, A.V., 2011. Effects of chlorpyrifos and chlorpyrifos-oxon on the dynamics and movement of mitochondria in rat cortical neurons. J. Pharmacol. Exp. Therap. 339, 341–349.

Miller, M.L., Chadwick, B., Dickstein, D.L., Purushothaman, I., Egervari, G., Rahman, T., et al, 2019. Adolescent exposure to Δ(9)-tetrahydrocannabinol alters the transcriptional trajectory and dendritic architecture of prefrontal pyramidal neurons. Mol. Psychiatry 24, 588–600.
Mohammed, A.N., Alugubelly, N., Kaplan, B.L., Carr, R.L., 2018. Effect of repeated juvenile exposure to Δ9-tetrahydrocannabinol on anxiety-related behavior and social interactions in adolescent rats. Neurotoxicol. Teratol. 69, 11–20.
Musshoff, F., Madea, B., 2006. Review of biologic matrices (urine, blood, hair) as indicators of recent or ongoing cannabis use. Ther. Drug Monit. 28, 155–163.
Mutch, E., Williams, F.M., 2006. Diazinon, chlorpyrifos and parathion are metabolised by multiple cytochromes P450 in human liver. Toxicology 224, 22–32.
Nair, A.B., Jacob, S., 2016. A simple practice guide for dose conversion between animals and human. J. Basic Clin. Pharmacy 7, 27–31.
Navarro, M., de Miguel, R., Rodríguez de fonseca, F., Ramos, J.A., Fernández-ruiz, J.J., 1996. Perinatal cannabinoid exposure modifies the sociosexual approach behavior and the mesolimbic dopaminergic activity of adult male rats. Behav. Brain Res. 75, 91–98.
Nebert, D.W., Dalton, T.P., Okey, A.B., Gonzalez, F.J., 2004. Role of aryl hydrocarbon receptor-mediated induction of the CYP1 enzymes in environmental toxicity and cancer. J. Biol. Chem. 279, 23847–23850.
Newsom, R.J., Kelly, S.J., 2008. Perinatal delta-9-tetrahydrocannabinol exposure disrupts social and open field behavior in adult male rats. Neurotoxicol. Teratol. 30, 213–219.
Nomura, D.K., Blankman, J.L., Simon, G.M., Fujioka, K., Issa, R.S., Ward, A.M., et al, 2008. Activation of the endocannabinoid system by organophosphorus nerve agents. Nat. Chem. Biol. 4, 373–378.
O'Shea, M., Mallet, P.E., 2005. Impaired learning in adulthood following neonatal delta9-THC exposure. Behav. Pharmacol. 16, 455–461.
O'Shea, M., McGregor, I.S., Mallet, P.E., 2006. Repeated cannabinoid exposure during perinatal, adolescent or early adult ages produces similar longlasting deficits in object recognition and reduced social interaction in rats. J. Psychopharmacol. 20 (5), 611–621.
OECD 2021a. Test No. 250: EASZY assay - Detection of Endocrine Active Substances, acting through estrogen receptors, using transgenic tg(cyp19a1b:GFP) Zebrafish embrYos.
OECD 2021b. Test No. 406: Skin Sensitisation.
OEHHA 2019. Evidence on the Developmental Toxicity of Cannabis (Marijuana) Smoke and Δ9-THC. Proposition 65, Reproductive and Cancer Hazard Assessment Branch.
Pallmann, P., Hothorn, L.A., 2016. Boxplots for grouped and clustered data in toxicology. Arch. Toxicol. 90, 1631–1638.
Pallotta, M.M., Ronca, R., Carotenuto, R., Porreca, I., Turano, M., Ambrosino, C., et al, 2017. Specific effects of chronic dietary exposure to chlorpyrifos on brain gene expression—a mouse study. Int. J. Mol. Sci. 18, 2467.
Payne, K.S., Mazur, D.J., Hotaling, J.M., Pastuszak, A.W., 2019. Cannabis and male fertility: a systematic review. J. Urol. 202, 674–681.
Pearce, R.G., Setzer, R.W., Strope, C.L., Sipes, N.S., Wambaugh, J.F., 2017. httk: R package for high-throughput toxicokinetics. J. Stat. Softw. 79, 1–26.
Peleg-Raibstein, D., Feldon, J., 2006. Effects of dorsal and ventral hippocampal NMDA stimulation on nucleus accumbens core and shell dopamine release. Neuropharmacology 51, 947–957.
Pertwee, R.G., 2006. The pharmacology of cannabinoid receptors and their ligands: an overview. Int. J. Obes. (Lond.) 30 (Suppl 1), S13–S18.
Pertwee, R.G., Howlett, A.C., Abood, M.E., Alexander, S.P.H., di Marzo, V., Elphick, M. R., et al, 2010. International union of basic and clinical pharmacology. LXXIX. Cannabinoid receptors and their ligands: beyond CB_1 and CB_2. Pharmacol. Rev. 62, 588–631.
Poleg, S., Golubchik, P., Offen, D., Weizman, A., 2019. Cannabidiol as a suggested candidate for treatment of autism spectrum disorder. Prog. Neuro-Psychopharmacol. Biol. Psychiatry 89, 90–96.
Pretzsch, C.M., Voinescu, B., Mendez, M.A., Wichers, R., Ajram, L., Ivin, G., et al, 2019. The effect of cannabidiol (CBD) on low-frequency activity and functional connectivity in the brain of adults with and without autism spectrum disorder (ASD). J. Psychopharmacol. 33 (9), 1141–1148.
Prior, H., Casey, W.M., Kimber, I., Whelan, M., Sewell, F., 2019. Reflections on the progress towards non-animal methods for acute toxicity testing of chemicals. Regul. Toxicol. Pharm. 102, 30–33.
Raber, J.C., Elzinga, S., Kaplan, C., 2015. Understanding dabs: contamination concerns of cannabis concentrates and cannabinoid transfer during the act of dabbing. J. Toxicol. Sci. 40, 797–803.
Rauh, V., Arunajadai, S., Horton, M., Perera, F., Hoepner, L., Barr, D.B., et al, 2011. Seven-year neurodevelopmental scores and prenatal exposure to chlorpyrifos, a common agricultural pesticide. Environ. Health Perspect. 119, 1196–1201.
Rauh, V.A., Garcia, W.E., Whyatt, R.M., Horton, M.K., Barr, D.B., Louis, E.D., 2015. Prenatal exposure to the organophosphate pesticide chlorpyrifos and childhood tremor. Neurotoxicology 51, 80–86. https://doi.org/10.1016/j.neuro.2015.09.004.
Rauh, V.A., Perera, F.P., Horton, M.K., Whyatt, R.M., Bansal, R., Hao, X., et al, 2012. Brain anomalies in children exposed prenatally to a common organophosphate pesticide. Proc. Natl. Acad. Sci. U.S.A. 109, 7871–7876.
Ring, C., Sipes, N.S., Hsieh, J.-H., Carberry, C., Koval, L.E., Klaren, W.D., et al, 2021. Predictive modeling of biological responses in the rat liver using in vitro Tox21 bioactivity: Benefits from high-throughput toxicokinetics. Comput. Toxicol. 18, 100166. https://doi.org/10.1016/j.comtox.2021.100166.
Ring, C.L., Pearce, R.G., Setzer, R.W., Wetmore, B.A., Wambaugh, J.F., 2017. Identifying populations sensitive to environmental chemicals by simulating toxicokinetic variability. Environ. Int. 106, 105–118.
Rubino, T., Realini, N., Braida, D., Guidi, S., Capurro, V., Viganò, D., et al, 2009. Changes in hippocampal morphology and neuroplasticity induced by adolescent THC treatment are associated with cognitive impairment in adulthood. Hippocampus 19, 763–772.
Sadler, N.C., Nandhikonda, P., Webb-Robertson, B.-J., Ansong, C., Anderson, L.N., Smith, J.N., et al, 2016. Hepatic cytochrome P450 activity, abundance, and expression throughout human development. Drug Metab. Dispos. 44, 984.
Saili, K.S., Antonijevic, T., Zurlinden, T.J., Shah, I., Deisenroth, C., Knudsen, T.B., 2020. Molecular characterization of a toxicological tipping point during human stem cell differentiation. Reprod. Toxicol. 91, 1–13.
Saili, K.S., Franzosa, J.A., Baker, N.C., Ellis-Hutchings, R.G., Settivari, R.S., Carney, E.W., et al, 2019. Systems modeling of developmental vascular toxicity. Curr. Opin. Toxicol. 15, 55–63.
Sams, C., Mason, H.J., Rawbone, R., 2000. Evidence for the activation of organophosphate pesticides by cytochromes P450 3A4 and 2D6 in human liver microsomes. Toxicol. Lett. 116, 217–221.
Seltenrich, N., Itenrich 2019. Into the weeds: regulating pesticides in cannabis. Environ. Health Perspect. 127, 042001.
Sengupta, P., 2011. A scientific review of age determination for a laboratory rat: how old is it in comparison with human age? Biomed. Int. 2, 81–89.
Sengupta, P., 2013. The laboratory rat: relating its age with human's. Int. J. Preventive Med. 4, 624–630.
Shelton, J.F., Geraghty, E.M., Tancredi, D.J., Delwiche, L., Schmidt, R.J., Ritz, B., et al, 2014. Neurodevelopmental disorders and prenatal residential proximity to agricultural pesticides: the CHARGE Study. Environ. Health Perspect. 122, 1103–1109.
Silva, M.H., 2020. Effects of low-dose chlorpyrifos on neurobehavior and potential mechanisms: a review of studies in rodents, zebrafish, and Caenorhabditis elegans. Birth Defects Research 112, 445–479.
Singh, N., Lawana, V., Luo, J., Phong, P., Abdalla, A., Palanisamy, B., et al, 2018. Organophosphate pesticide chlorpyrifos impairs STAT1 signaling to induce dopaminergic neurotoxicity: implications for mitochondria mediated oxidative stress signaling events. Neurobiol. Dis. 117, 82–113.
Sipes, N.S., Wambaugh, J.F., Pearce, R.G., Auerbach, S.S., Wetmore, B.A., Hsieh, J.-H., et al, 2017. An intuitive approach for predicting potential human health risk with the Tox21 10k library. Environ. Sci. Technol. 51, 10786–10796.
Slotkin, T., Seidler, F., 2007. Prenatal chlorpyrifos exposure elicits presynaptic serotonergic and dopaminergic hyperactivity at adolescence: critical periods for regional and sex-selective effects. Reprod. Toxicol. 23 (3), 421–427.
Slotkin, T.A., Seidler, F.J., 2009. Oxidative and excitatory mechanisms of developmental neurotoxicity: transcriptional profiles for chlorpyrifos, diazinon, dieldrin, and divalent nickel in PC12 Cells. Environ. Health Perspect. 117, 587–596.
Slotkin, T.A., Seidler, F.J., 2010. Diverse neurotoxicants converge on gene expression for neuropeptides and their receptors in an in vitro model of neurodifferentiation: effects of chlorpyrifos, diazinon, dieldrin and divalent nickel in PC12 cells. Brain Res. 1353, 36–52.
Slotkin, T.A., Skavicus, S., Levin, E.D., Seidler, F.J., 2020. Paternal Δ9-tetrahydrocannabinol exposure prior to mating elicits deficits in cholinergic synaptic function in the offspring. Toxicol. Sci. 174, 210–217.
Snider, N.T., Walker, V.J., Hollenberg, P.F., 2010. Oxidation of the endogenous cannabinoid arachidonoyl ethanolamide by the cytochrome P450 monooxygenases: physiological and pharmacological implications. Pharmacol. Rev. 62, 136–154.
Stella, N., 2009. Endocannabinoid signaling in microglial cells. Neuropharmacology 56 (Suppl 1), 244–253.
Stempfer, M., Reinstadler, V., Lang, A., Oberacher, H., 2021. Analysis of cannabis seizures by non-targeted liquid chromatography-tandem mass spectrometry. J. Pharm. Biomed. Anal. 205, 114313.
Tamási, V., Vereczkey, L., Falus, A., Monostory, K., 2003. Some aspects of interindividual variations in the metabolism of xenobiotics. Inflamm. Res. 52, 322–333.
Tan, Y.M., Liao, K.H., Clewell III, H.J., 2007. Reverse dosimetry: Interpreting trihalomethanes biomonitoring data using physiologically based pharmacokinetic modeling. J. Expo. Sci. Environ. Epidemiol. 17, 591–603.
Tau, G.Z., Peterson, B.S., 2010. Normal development of brain circuits. Neuropsychopharmacology 35, 147–168.
Taylor, A., Birkett, J.W., 2020. Pesticides in cannabis: a review of analytical and toxicological considerations. Drug Test. Anal. 12, 180–190.
Testai, E., Buratti, F.M., Di Consiglio, E., 2010. Chapter 70: Chlorpyrifos. In: Hayes' Handbook of Pesticide Toxicology. Elsevier, pp. 1505–1526.
Trezza, V., Campolongo, P., Cassano, T., Macheda, T., Dipasquale, P., Carratù, M.R., et al, 2008. Effects of perinatal exposure to delta-9-tetrahydrocannabinol on the emotional reactivity of the offspring: a longitudinal behavioral study in Wistar rats. Psychopharmacology 198 (4), 529–537.
US EPA 1998. Health effect Test Guidelines (OPPS 870). Prevention, Pesticides and Toxic Substances (7101), U.S. Environmental Protection Agency, Washington, DC (https://www.epa.gov/test-guidelines-pesticides-and-toxic-substances/series-870-health-effects-test-guidelines; accessed 3/2020).
US EPA 2011. Chlorpyrifos: Preliminary Human Health Risk Assessment for Registration Review. Office of Chemical Safety and Pollution Prevention, United States Environmental Protection Agency, Washington D.C., https://www.regulations.gov/document?D = EPA-HQ-OPP-2008-0850-0025 (accessed 3-2020), 1–159.
US EPA 2020a. Chlorpyrifos: Third Revised Human Health Risk Assessment for Registration Review. Office of Chemical Safety and Pollution Prevention, U.S. Environmental Protection Agency, Washington, DC., EPA-HQ-OPP-2008-0850-944.

US EPA, 2020b. EPA New Approach Methods: Efforts to Reduce Use of Animals in Chemical Testing. https://www.epa.gov/research/epa-new-approach-methods-efforts-reduce-use-animals-chemical-testing; Accessed October, 2020.

Vela, G., Martı´n, S., Garcı´a-Gil, Lucı´a, Crespo, J.A., Ruiz-Gayo, M., Javier Fernández-Ruiz, J., et al, 1998. Maternal exposure to Δ9-tetrahydrocannabinol facilitates morphine self-administration behavior and changes regional binding to central μ opioid receptors in adult offspring female rats. Brain Res. 807 (1-2), 101–109.

Viswakarma, N., Jia, Y., Bai, L., Vluggens, A., Borensztajn, J., Xu, J., et al, 2010. Coactivators in PPAR-regulated gene expression. PPAR Res. 2010, 1–21.

Voelker, R., Holmes, M., 2015. Pesticide Use on Cannabis. Cannabis Safety Institute, Eugene, OR, pp. 1–19.

Vyhlidal, C.A., Gaedigk, R., Leeder, J.S., 2006. Nuclear receptor expression in fetal and pediatric liver: correlation with Cyp3a expression. Drug Metab. Dispos. 34, 131.

Wambaugh, J., Pearce, P., Ring, C., Davis, J., Sipes, N., Setzer, W. R. 2019. Package 'httk' (httk.pdf) [Online]. https://cran.r-project.org/web/packages/httk/index.html. Available: https://www.epa.gov/chemical-research/rapid-chemical-exposure-and-dose-research [Accessed 10-17 2019].

Wambaugh, J., Pearce, R., Ring, C., Honda, G., Sfeir, M., Davis, J., Sluka, J. P., Sipes, N., Wetmore, B.A., Setzer, W. 2021. httk: High-Throughput Toxicokinetics [Online]. [Accessed 8-2021].

Wambaugh, J.F., Wetmore, B.A., Pearce, R., Strope, C., Goldsmith, R., Sluka, J.P., et al, 2015a. Toxicokinetic triage for environmental chemicals. Toxicol. Sci. 147 (1), 55–67.

Wambaugh, J., Wetmore, B.A., Pearce, R.G., Strope, C., Goldsmith, M.-R., Sluka, J., et al, 2015b. Toxicokinetic triage for environmental chemicals. Toxicol. Sci. 147, 55–67.

Wambaugh, J.F., Hughes, M.F., Ring, C.L., Macmillan, D.K., Ford, J., Fennell, T.R., et al, 2018. Evaluating in vitro-in vivo extrapolation of toxicokinetics. Toxicol. Sci. 163, 152–169.

Wang, H., Negishi, M., 2003. Transcriptional regulation of cytochrome P450 2B genes by nuclear receptors. Curr. Drug Metab. 4, 515–525.

Wang, X., Dow-Edwards, D., Anderson, V., Minkoff, H., Hurd, Y.L., 2006. Discrete opioid gene expression impairment in the human fetal brain associated with maternal marijuana use. Pharmacogenomics J. 6, 255–264.

Wang, X., Dow-Edwards, D., Keller, E., Hurd, Y., 2003. Preferential limbic expression of the cannabinoid receptor mRNA in the human fetal brain. Neuroscience 118, 681–694.

Weldon, R.H., Barr, D.B., Trujillo, C., Bradman, A., Holland, N., Eskenazi, B., 2011. A pilot study of pesticides and PCBs in the breast milk of women residing in urban and agricultural communities of California. J. Environ. Monit. 13, 3136–3144.

WHO, 2017. Guidance document on evaluating and expressing uncertainty in hazard characterization. World Health Organization, Geneva, Switzerland, https://apps.who.int/iris/bitstream/handle/10665/259858/9789241513548-eng.pdf;sequence=1#:~:text=GUIDANCE%20DOCUMENT%20ON%20EVALUATING%20AND%20EXPRESSING%20UNCERTAINTY%20IN,sponsorship%20of%20the%20World%20Health%20Organization%2C%20the%20International; accessed 3-2020), xxii + 159 pp.

Williams, A.J., Grulke, C.M., Edwards, J., McEachran, A.D., Mansouri, K., Baker, N.C., et al, 2017. The CompTox Chemistry Dashboard: a community data resource for environmental chemistry. J. Cheminform. 9 (1). https://doi.org/10.1186/s13321-017-0247-6.

Woods, C.G., Vanden Heuvel, J.P., Rusyn, I., 2007. Genomic profiling in nuclear receptor-mediated toxicity. Toxicol. Pathol. 35, 474–494.

Wylie, P.L., Westland, J., Wang, M., Radwan, M.M., Majumdar, C.G., Elsohly, M.A., 2020. Screening for More than 1,000 pesticides and environmental contaminants in cannabis by GC/Q-TOF. Med. Cannabis Cannabinoids 3, 14–24.

Zamberletti, E., Rubino, T., 2021. Impact of endocannabinoid system manipulation on neurodevelopmental processes relevant to schizophrenia. Biol. Psychiatry: Cognitive Neurosc. Neuroimag. 6, 616–626.

Zendulka, O., Dovrtelová, G., Nosková, K., Turjap, M., Sulcová, A., Hanus, L., et al, 2016. Cannabinoids and cytochrome P450 interactions. Curr. Drug Metab. 17, 206–226.

Zou, S., Kumar, U., 2018. Cannabinoid receptors and the endocannabinoid system: signaling and function in the central nervous system. Int. J. Mol. Sci. 19 (3), 833. https://doi.org/10.3390/ijms19030833.